รายงานค<mark>วาม</mark>ก้าวหน้าโครงการ ในรอบ 18 เดือน สำนักงานกองทุนสนับสนุนการวิจัย (สกว.) สัญญาเลขที่ RSA/20/2540

ชื่อโครงการวิจัย (ภาษาไทย) :

ระบบไม่เชิงเส้นในการจำลองทางคณิตศาสตร์

เชิงนิเวศน์วิทยา : ระบบรวมและระบบแยก

(ภาษาอังกฤษ) :

Nonlinear Systems in Ecological Modelling:

Coupled and Decoupled Systems

ได้รับทุนอุดหนุนการวิจัยประเภท ทุนพัฒนานักวิจัย ประจำปี 2540

สัญญาเลขที่ RSA/20/2540 ทุนพัฒนานักวิจัย

รายงานสรุปความก้าวหน้าของโครงการในรอบ 18 เดือน

รายงานในช่วงตั้งแต่วันที่ 1 ธันวาคม 2540

ถึงวันที่ 31 พฤษภาคม 2542

ชื่อหัวหน้าโครงการ: นาง ยงค์วิมล เลณบุรี

หน่วยงาน :

ภาควิชาคณิตศาสตร์ คณะวิทยาศาสตร์ มหาวิทยาลัยมหิดล

1. การดำเนินงาน:

ได้ดำเนินงานตามแผนงานที่ได้วางไว้ทุกประการ

ใค้เปลี่ยนแปลงแผนงานที่ได้วางไว้คังนี้คือ

ตารางกิจกรรมตามแผนงานของโครงการ

กิจกรรม	เดือนที่					
	1-3	4-6	7-9	10-12	13-15	16-18
1. ค้นคว้าศึกษาเอกสารอ้างอิง	<·····	>				
	←					
2. วิเคราะห์วิจัยแบบจำลองที่ coupled และ	!	<			· · · · >	
decoupled ด้วยทฤษฎีทางคณิตศาสตร์						
แล้วตรวจสอบผลด้วย computer simulation						
และข้อมูลสนาม						
3. ศึกษาและใช้ decoupling theory กับแบบ		1			<·····	
จำลองของระบบที่ศึกษาเพื่อความรู้ทางด้าน					←	
management และ control แล้วตรวจสอบผล						
ค้วย computer simulation และข้อมูลสนาม						

กิจกรรมตามแผนงาน

กิจกรรมที่ดำเนินงานแล้ว

2. สรุปผลการดำเนินงาน

ช่วง 12 เดือนแรก

ผู้วิจัยได้ดำเนินงานวิจัยเกี่ยวกับการจำลองจลศาสตร์ (dynamical modelling) ของ coupled systems ในเชิงนิเวศน์วิทยาตามที่เสนอไว้ โดยให้ความสนใจเป็นพิเศษกับระบบของ ผู้ล่า-เหยื่อ ซึ่งได้รับ ผลกระทบจากการติดเชื้อหรือพยาธิ รวมทั้งกระบวนการ activated sludge ซึ่งถูก coupled โดย membrane permeability หรือจากระดับของ substrate และ product ตามที่ได้รายงานไว้แล้วในแบบรายงาน ความก้าวหน้าโครงการในรอบ 12 เดือน

จนกระทั่งขณะนี้ papers ทั้ง 2 ฉบับที่ได้ submit ไปนั้น ฉบับหนึ่งได้ published แล้ว ส่วนอีก ฉบับหนึ่งได้คำตอบรับ (accepted) ให้ตีพิมพ์ในวารสารวิชาการแล้ว หลังจากทำการแก้ไขและเพิ่มเติม รายละเอียดบางส่วนตามคำแนะนำของ readers (กรุณาดู ข้อ 5. สรุป output ของโครงการ) ตามที่ได้ แนบมาเป็นเอกสารประกอบการพิจารณา อันดับที่ 1 และ 2 ตามลำดับ

ช่วง 6 เคือนหลัง

ผู้วิจัยได้เริ่มดำเนินการวิจัยในเชิง control เพื่อแยก (decouple) ระบบโซ่ใยอาหาร (food web) ให้ การเปลี่ยนแปลงในระดับของตัวแปรหนึ่ง ถูกแยกออกจากการเปลี่ยนแปลงในระดับของตัวแปรอื่นๆ เช่น ระดับของเหยื่อ (prey) จะถูกควบคุมให้คงที่ได้ ในขณะที่มีความเปลี่ยนแปลงในระดับของ predator และ superpredator

เราใช้ static state-feedback decoupling theory ในการหาเงื่อนไขที่จะสามารถ decouple ระบบ โซ่ใยอาหาร ซึ่งจำลองด้วยแบบจำลองแบบ Komolgorov โดยที่เราสามารถแสดงได้ว่าแบบจำลอง ดังกล่าวสามารถแสดงพฤติกรรมที่สับสน (chaotic behavior) ได้ สำหรับค่าของพารามิเตอร์ในช่วง บางช่วง แต่เมื่อใช้ control law ซึ่งเราสร้างขึ้นมานั้นแล้ว พบว่าเราสามารถ control ระบบที่สับสนให้ ระดับของตัวแปรหนึ่งถูกควบคุมให้คงที่ได้ ในขณะที่ตัวแปรอื่นๆ มีความเปลี่ยนแปลงอย่างแปรปรวน (irregular)

นอกไปจากนั้นเรายังแสดงได้ด้วยว่า control law จะ exist ก็ต่อเมื่อประชากรของเหยื่อ persist นั่นคือไม่สูญพันธุ์ไป ณ ขณะใคขณะหนึ่ง รวมทั้งอัตราการเจริญเติบโตสัมพัทธ์ของเหยื่อจะต้องขึ้นกับ ระดับของ superpredator อย่างชัดแจ้ง (explicit)

ผู้วิจัยได้นำผลงานวิจัยในช่วงนี้เขียนขึ้นเป็น paper และ submitted for publication แล้ว ใน Journal of Theoretical Biology ดังที่จะสามารถดูรายละเอียดได้ในเอกสารที่แนบมาประกอบการ พิจารณา อันดับที่ 3

การดำเนินงาน ยังไม่พบอุปสรรคแต่อย่างใด

4. ข้อคิดเห็นและข้อเสนออื่น ๆ ต่อ สกว.

ไม่มี

5. สรุป output ของโครงการ

- 5.1 Lenbury, Y., Puttapiban, P., and Amornsamankul, S. Modelling Effects of High Product and Substrate Inhibition on Oscillatory Behavior in Continuous Bioreactors. *BioSystems*. 49 (1999) 191-203.
- 5.2 Lenbury, Y., Rattanamongkonkul, S., Tumrasvin, N., and Amornsamankul, S. Predator prey Interaction Coupled by Parasitic Infection: Limit Cycles and Chaotic Behavior. Mathematical and Computer Modelling. In press.
- 5.3 Lenbury, Y., and Kettapun, A. Modelling the Effect of Membrane Permeability on the Dynamics of a Continuous Bio - Reactor: Investigating Bifurcation and Chaotic Behavior. Proceedings of the Second Annual National Symposium on Computational Science and Engineering, March 26 - 27, 1998, NSTDA.
- 5.4 Lenbury, Y., Pansuwan, A., Tumrasvin, N. Chaos and Control Action in a Kolmogorov Type Model for Food Webs with Harvesting or Replenishment. *Journal of Theoretical Biology*. Submitted.

ลงนาม รวลจับบุริ (หัวหน้าโครงการ) เอกสารประกอบอันดับที่ 1



BioSystems 49 (1999) 191-203



Modelling effects of high product and substrate inhibition on oscillatory behavior in continuous bioreactors

Yongwimon Lenbury *, Apichat Neamvong, Somkid Amornsamankul, Pannee Puttapiban

Department of Mathematics, Faculty of Science, Mahidol University, Rama 6 Rd., Bangkok 10400, Thailand

Received 24 February 1998; received in revised form 11 August 1998; accepted 11 August 1998

Abstract

In this study we consider a model for continuous bioreactors which incorporates the effects of high product and substrate inhibition on the kinetics as well as biomass and product yields. We theoretically investigate the possibility of various dynamic behaviors in the bioreactor over different ranges of operating parameters to determine the delineating process conditions which may lead to oscillatory behavior. Application of the singular perturbation technique allows us to derive explicit conditions on the system parameters which specifically ascertain the existence of limit cycles composed of concatenations of catastrophic transitions occurring at different speeds. We discover further that the interactions between the limiting substrate and the growing microorganisms can give rise to high frequency oscillations which can arise during the transients toward the attractor or during the low-frequency cycle. Such a study not only can describe more fully the kinetics in a fermentor but also assist in formulating optimum fermentor operating conditions and in developing control strategy for maintaining optimum productivity. © 1999 Elsevier Science Ireland Ltd. All rights reserved.

Keywords: Continuous bioreactors; Product inhibition; Substrate inhibition; Singular perturbation; Oscillation

1. Introduction

The growth of microorganisms is an unusually complicated phenomenon. Viewing the behavior of microbial cultures within the framework of lumped kinetic models, a multitude of models have been proposed and theoretically studied in diverse ways since the model due to Monod (1942), fashioned after Michaelis—Menten kinetics for single enzyme-substrate reactions.

In ethanol fermentation, instantaneous biomass yield of the yeast *Saccharomyces cerevisiae* was found by Thatipamala et al. (1992) to decrease with the increase in ethanol concentration (*P*),

^{*} Corresponding author. E-mail: scylb@mahidol.ac.th

indicating a definite relationship between biomass yield and product inhibition. Thatipamala et al. (1992) also found that substrate inhibition occurs when substrate concentration (S) is above 150 g/l. Fig. 1 shows experimental data taken from the work of Thatipamala et al. (1992) indicating the effect of substrate inhibition on the specific growth rate at low ethanol concentrations. Fig. 2, on the other hand, shows the effect of product inhibition on the specific growth rate, with data taken from the same source (Thatipamala et al., 1992).

A number of simple kinetic expressions have been suggested in the literature for specific growth rate μ incorporating product and/or substrate inhibition (Aiba and Shoda, 1969; Andrews, 1968; Bazua and Wilke, 1977). Mainly, four types of inhibition correlations have been suggested based on experimental observations: linear, exponential, hyperbolic, and parabolic. Yano and Koga (1969) made a theoretical study of the behavior of a single-vessel continuous fermentation subject to a growth inhibition at high concentration of the rate limiting substrate S. They used the following expression for their continuous fermentation system:

$$\mu = \frac{\mu_{\rm m}}{(K_{\rm s}/S) + 1 + \sum_{j=1}^{n} (S/K_{\rm j})^{j}}$$
(1)

where $\mu_{\rm m}$ and the K's are positive constants and n is a positive integer. Other workers (Agrawal et al., 1982; Lenbury et al., 1994) have adopted simpler specific growth rate functions involving fewer control parameters, but exhibiting similar characteristics as the usual substrate inhibition model, for example the one hump substrate inhibition function

$$\mu = k \operatorname{Se}^{-S/K_{s}} \tag{2}$$

where k and K_s are positive constants.

Later, Yano and Koga (1973) discussed the nature of the chemostat in which the specific growth rate depends on the concentrations of both a substrate and an inhibitory product of a microorganism. They assumed a specific growth rate equation as follows;

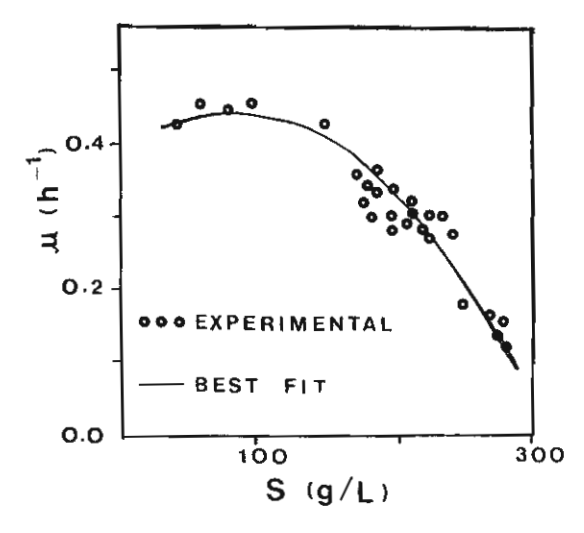


Fig. 1. Effect of substrate inhibition on specific growth rate at low ethanol concentration. (Data points taken from reference Aiba and Shoda (1969)).

$$\mu = \frac{\mu_{\rm m} S}{(K_{\rm s} + S) \left\{ 1 + \left(\frac{P}{K_{\rm p}}\right)^n \right\}} \tag{3}$$

They showed, with the analog computer, that when the product formation was negatively growth-associated, in which the rate of product formation decreases with the increase in the cells concentration, diverging as well as damped oscillations appeared. No oscillations could be ob-

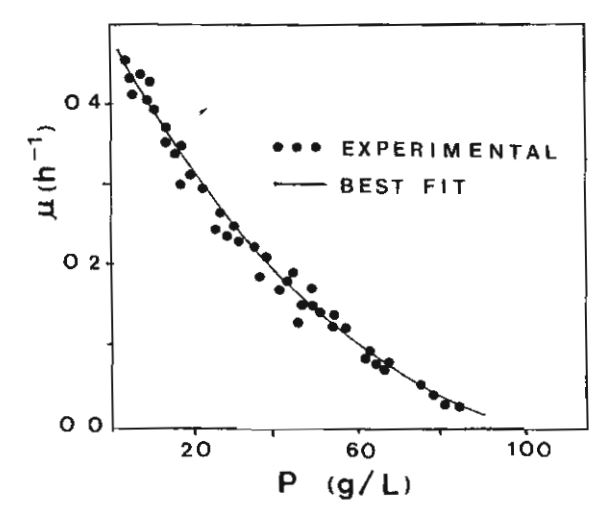


Fig. 2. Effect of product inhibition on specific growth rate. (Data points taken from reference Aiba and Shoda (1969)).

served, on the other hand, when the product formation was either completely growth-associated, or partially growth-associated. Oscillation phenomena are, however, not unusual in continuous cultures (Agrawal et al., 1982). Since a tendency for periodicity is undesirable from the point of view of process control, it is necessary to identify the safe operating regions in which complexed dynamic behavior may be avoided.

In one of their earlier efforts, Ramkrishna et al. (1967) presented a chemostat model which assumed that viable cells (X) interact with a substrate (S) so as to produce new viable cells and a cell-killing product (P). This product interacts with viable cells to form dead cells, in the process of which the cell-killing product may be released.

In the work of Lenbury et al. (1994), the dynamic behavior of a chemostat subject to product inhibition was analyzed and classified in terms of multiplicity and stability of steady states and limit cycles. The substrate was assumed to be in sufficient supply so that the model was reduced to a system of two nonlinear differential equations involving only the cells and product concentrations.

In this paper, we consider the full three-variable product inhibition model consisting of the following nonlinear differential equations:

$$\frac{\mathrm{d}X}{\mathrm{d}t} = \mu X - DX\tag{4}$$

$$\frac{\mathrm{d}S}{\mathrm{d}t} = D(S_1 - S) - \frac{\mu}{Y}X\tag{5}$$

$$\frac{\mathrm{d}P}{\mathrm{d}t} = \eta_0 \mu X + \eta_1 P - DP \tag{6}$$

where X(t) denotes the cells concentration at time t; S(t) the substrate concentration at time t; P(t) the product concentration at time t; S_F the concentration of the feed substrate, while D is the dilution rate at which the feed substrate is being fed into the reactor and the content of the bio-reactor is being removed, and η_0 is the constant for product formation. The term $\eta_1 P$ in equation (6) takes into account the release of the cell-killing product during the product's interaction with viable cells to form dead cells, following the suggestion of Ramkrishna et al. (1967) in their earlier mentioned paper. Here, we assume that the pro-

duction rate is directly proportional to the amount of the product present, with $\eta_1 < D$ being the positive constant of variation.

We also adopt the following expression for the specific growth rate function:

$$\mu = \frac{kSe^{-a}\frac{s}{s_{+}}}{1 + \frac{P}{K_{p}}} \tag{7}$$

to take into account the inhibitory effects of both the substrate and the product increase in the chemostat.

Further, the cells to substrate yield Y defined as

$$Y \equiv \frac{\text{amount of cells produced}}{\text{amount of substrate consumed}}$$

is assumed to vary linearly with the substrate level at any time t, allowing for the positively-growth associated situation; namely

$$Y = A + BS \tag{8}$$

Such substrate dependent yield has been used previously by several other workers in this field (Agrawal et al., 1982; Lenbury et al., 1994).

The analysis of the model is done through a singular perturbation argument, assuming that the substrate concentration exhibits fast dynamics. The time responses of the different components in the system are assumed to decrease dynamically from top to bottom. The structure of the corresponding attractors and the nature of the transients are then analyzed. It is shown that the model system can exhibit low-frequency cycles in which periodic bursts of high-frequency oscillations may develop giving rise to more complexed dynamical behavior for specified ranges of the system parameters.

2. System model

In order to analyze the model system of Eqs. (4)–(6), together with Eqs. (7) and (8) through the singular perturbation technique, we assume that the substrate has fast dynamics, while the cells and product have intermediate and slow dynamics respectively, and scale the time responses of the

three hierarchical components of the system by means of two small dimensionless positive parameters ε and δ ; namely, we let

$$x = \frac{S}{S_{\rm F}}, \quad y = X, \quad z = \frac{P}{\varepsilon K_{\rm p}}, \quad d_1 = D, \quad d_2 = \frac{D}{\varepsilon},$$
$$d_3 \frac{D - \eta_1}{\varepsilon \delta}, \quad \omega = \frac{k S_{\rm F}}{\varepsilon K_{\rm p}}, \quad \eta = \frac{\eta_0 \omega}{\varepsilon \delta}, \quad \gamma = \frac{k}{A S_{\rm F}},$$
and $\beta = \frac{A}{B S_{\rm F}}$.

We are led to the following system of differential equations:

$$\frac{\mathrm{d}x}{\mathrm{d}t} = d_1(1-x) - \frac{\gamma x \,\mathrm{e}^{-\alpha x} y}{(x+\beta)(1+\varepsilon z)} \equiv f(x,y,z) \qquad (9)$$

$$\frac{\mathrm{d}y}{\mathrm{d}t} = \varepsilon y \left[\frac{\omega x \, \mathrm{e}^{-ax}}{1 + \varepsilon z} - d_2 \right] \equiv \varepsilon g(x, y, z) \tag{10}$$

$$\frac{\mathrm{d}z}{\mathrm{d}t} = \varepsilon \delta \left[\frac{\eta x \, \mathrm{e}^{-\alpha x}}{1 + \varepsilon z} \, y - d_3 z \, \right] \equiv \varepsilon \delta h(x, y, z) \tag{11}$$

Thus, with ε and δ small, the equation of the substrate concentration represents the fast system, while that of the cells and product concentrations represent the intermediate and the slow systems, respectively. Under suitable regularity assumptions, the singular perturbation method allows us to approximate the solution of the system (Eqs. (9)-(11)) with a sequence of simple dynamic transitions along the various equilibrium manifolds of the system and occurring at different speeds. The resulting path, composed of all such transients, approximates the solution of the system in the sense that the real trajectory is contained in a tube around these transients, and that the radius of the tube goes to zero with ε and δ . The formal proof of this is not given because it is long and trivial and has already been discussed and extensively used in the literature (Hoppensteadt, 1974; Muratori and Rinaldi, 1989; Muratori, 1991; Muratori and Rinaldi, 1992).

2.1. Two-dimensional dynamics

By means of singular perturbation analysis, the solution of the system of Eqs. (9)–(11) can be approximately found for small values of ε and δ . First, the slow (z) and intermediate (y) variables are frozen at their initial values z(0) and y(0), and

the evolution of the fast component of the system is determined by solving the 'fast system' consisting of Eq. (9) with z set equal to z(0). If, for simplicity of the following analysis, we assume that the starting value of z is comparatively small, since δ is small, the value of z remains small during the initial phase. The evolution of the system components can then be approximately determined by first setting $\delta = 0$ and z = 0 in the Eqs. (9)–(11). Thus, we are led to the following system:

$$\frac{\mathrm{d}x}{\mathrm{d}t} = d_1(1-x) - \frac{\gamma x \,\mathrm{e}^{-ax}y}{(x+\beta)} \tag{12}$$

$$\frac{\mathrm{d}y}{\mathrm{d}t} = \varepsilon y \left[\omega x \, \mathrm{e}^{-\alpha x} - d_2\right] \tag{13}$$

which is a fast-slow second-order system for which the dynamical behavior can be analyzed and existence of limit cycles detected through the singular perturbation principle. The results are summarized in Fig. 3, where two cases of interest can be identified. The conditions on the parameters identifying the two cases are as follows.

2.1.1. Case 1

The system (Eq. (12)) has an equilibrium manifold where $\dot{x} = 0$ is given by

$$y = (1 - x)(x + \beta) \frac{e^{ax}}{yx} \equiv \varphi(x)$$
 (14)

which intersects the x-axis at the point x = 1 as shown in Fig. 3. The slope of the curve in Eq. (14) is given by

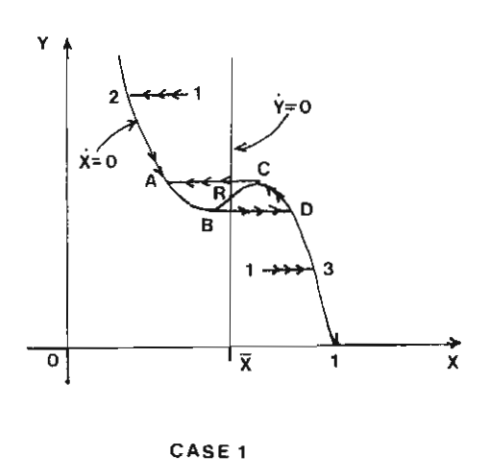
$$\frac{\mathrm{d}y}{\mathrm{d}x} = \frac{\mathrm{e}^{ax}}{\gamma x^2} F(x)$$

$$\equiv \frac{\mathrm{e}^{ax}}{\gamma x^2} [-ax^3 + (a - a\beta - 1)x^2 + a\beta x - \beta]$$
(15)

Letting x = 1/3 in Eq. (15) leads to the following inequality

$$\beta < \frac{2a-3}{27-6a} \tag{16}$$

which ensures that the curve $y = \varphi(x)$ has positive slope on some interval containing the point x = 1/3. On such an interval, the fast manifold f = 0 will be unstable. This corresponds to the portion BC in Fig. 3. Since f < 0 to the left of BC and f > 0 to



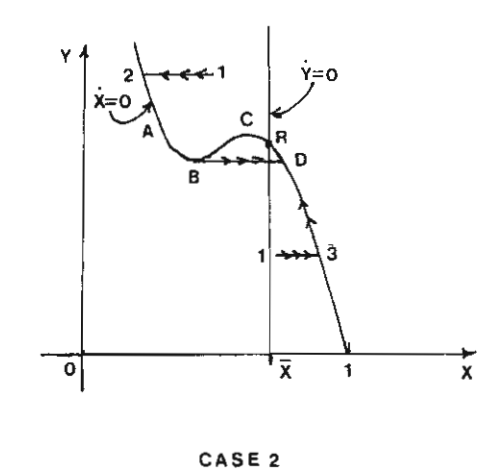


Fig. 3. Two possible cases of trajectory development for the two dimensional fast-slow system (Eqs. (12) and (13)). Trajectories go toward a limit cycle ABDC in Case 1, and toward a stable equilibrium point R in Case 2.

its right, a solution trajectory starting from a point to the left of this portion BC of the curve will develop away from the curve, while a trajectory starting from a point to the right of BC will tend away from this unstable branch of the curve also.

Similar arguments will show that the other branches of the manifold f = 0 on which we find the portions AB and CD are stable. The stability of different parts of other manifolds can be determined in a similar manner by considering the signs of the functions f, g and h.

The equilibrium manifold of the intermediate system (Eq. (13)) consists of 2 parts, the trivial manifold y = 0 and the nontrivial manifold given by the equation

$$x e^{-ax} = \frac{d_2}{\omega} \tag{17}$$

In the case 1, the curve (Eq. (17)) intersects the graph of (Eq. (14)) at the point R in the Fig. 3 where $x = \tilde{x}$ for which

$$F(\bar{x}) > 0 \tag{18}$$

which means that the point R is located on the unstable branch of the manifold f = 0. This is easily accomplished by letting

$$\tilde{x} = \frac{1}{3} - \theta \tag{19}$$

for a sufficiently small θ , then simply set

$$\frac{d_2}{\omega} = \bar{x} e^{-\bar{x}} = \left(\frac{1}{3} - \theta\right) e^{-(1/3 - \theta)} \tag{20}$$

Thus, Case 1 is identified by the inequality Eqs. (18)-(20).

2.1.2. Case 2

This case is then identified by the opposite inequality to Eq. (18), namely

$$F(\bar{x}) < 0 \tag{21}$$

However, since the nontrivial intermediate manifold is given by Eq. (17),

$$\bar{x} > \frac{d_2}{\omega}$$
 (22)

We see that Eq. (21) will be satisfied if d_2/ω is sufficiently large as well as satisfying

$$\frac{d_2}{\omega} < 1 \tag{23}$$

to allow for \bar{x} to be located to the left of the point x = 1 where the fast manifold crosses the x-axis.

Thus, in Fig. 3 where transitions of low, intermediate, and high speeds are indicated by one, two, and three arrows, respectively, if we start from the point marked by the number 1 above the curve $\dot{x} = 0$, then $\dot{x} < 0$ here and a fast transition develops toward the point 2 on the stable mani-

fold (section AB), while y still remains frozen at the initial value y(0). (If we start from the point 1 below the curve $\dot{x} = 0$, then $\dot{x} > 0$ here and so a fast transition will develop toward point 3 on section CD of the manifold). Since the manifold is stable here, a transition of intermediate speed is made along the curve as the intermediate system becomes active. From point 2, the transition develops along the direction of decreasing v since $\dot{y} < 0$ on the left of the curve g = 0. Once the point B is reached, the manifold loses its stability and a fast transition is made towards the point D on the stable section CD of the manifold. Transition of intermediate speed upwards along this curve ends if either a stable equilibrium R, where f = g = 0, is reached in the case 2 (Fig. 3b), or a quick jump brings the trajectory back to the section AB completing a closed cycle ABDC in the case 1 which corresponds to Fig. 3a.

2.2. Three-dimensional dynamics

As z increases, the slow system (Eq. (11)) becomes active. We now show that, for suitable values of the parameters and for ε and δ sufficiently small, the system (Eqs. (9)–(11)) has a unique attractor that is either a stable equilibrium or a low-frequency limit cycle which may exhibit high-frequency oscillations during a finite interval of time.

To do this, we observe that the manifold

$$f(x, y, z) = 0 \tag{24}$$

intersects the nontrivial intermediate manifold along the curve

$$f = g = 0 \tag{25}$$

given by the equation

$$\frac{x e^{-ax}}{1 + \varepsilon z} = \frac{d_2}{\omega} \tag{26}$$

which defines a surface $z = \psi(x)$. We observe that at x = 1/a

$$\frac{\mathrm{d}z}{\mathrm{d}x} = 0$$

Thus, to ensure that the point $P(z_p, y_p, z_p)$ in Fig. 4 is located on the stable part of the manifold f = 0 at the point where $x_p = 1/a < 1$, we require

$$F\left(\frac{1}{a}\right) < 0 \tag{27}$$

or equivalently,

$$\beta > 1 - \frac{1}{a} - \frac{1}{a^2} \tag{28}$$

and

$$a > 1$$
 (29)

Combining the Eq. (16) and Eq. (28), we arrive at the requirement that

$$\frac{2a-3}{27-6a} > \beta > 1 - \frac{1}{a} - \frac{1}{a^2} \tag{30}$$

Now, the curve (Eq. (25)) is given by the equation

$$y = \frac{d_2}{\omega}(1 - x)(x + \beta)$$

which reaches a maximum at the point $M(x_M, y_M, z_M)$ where

$$x_{\mathbf{M}} = \frac{1 - \beta}{2}$$

Finally, the curve f = g = 0 intersects the (x, z)plane at the point $O(x_O, y_O, z_O)$ where $x_O = 1$ and, from (Eq. (26)),

$$z_O = \frac{1}{\varepsilon} \left(\frac{\omega}{d_2 e^a} - 1 \right) \tag{31}$$

We therefore require that

$$e^{u} < \frac{\omega}{d_2} \tag{32}$$

to ensure that $z_{o} > 0$.

We now analyze each of the two cases separately.

2.2.1. Case 1

We observe that in this case the point R is located on the unstable part of the manifold f=0 and the curve f=g=0 remains on the unstable part, as shown in Fig. 4, until the point M is reached. The curve then stretches along the stable part of the manifold f=0 until either the point S is reached in the cases I(a) and I(b) (Fig. 4a, b), respectively), or the point P is reached first in the cases I(c) and I(d) (Fig. 4c, d), respectively). Thus, four subcases can be identified as follows.

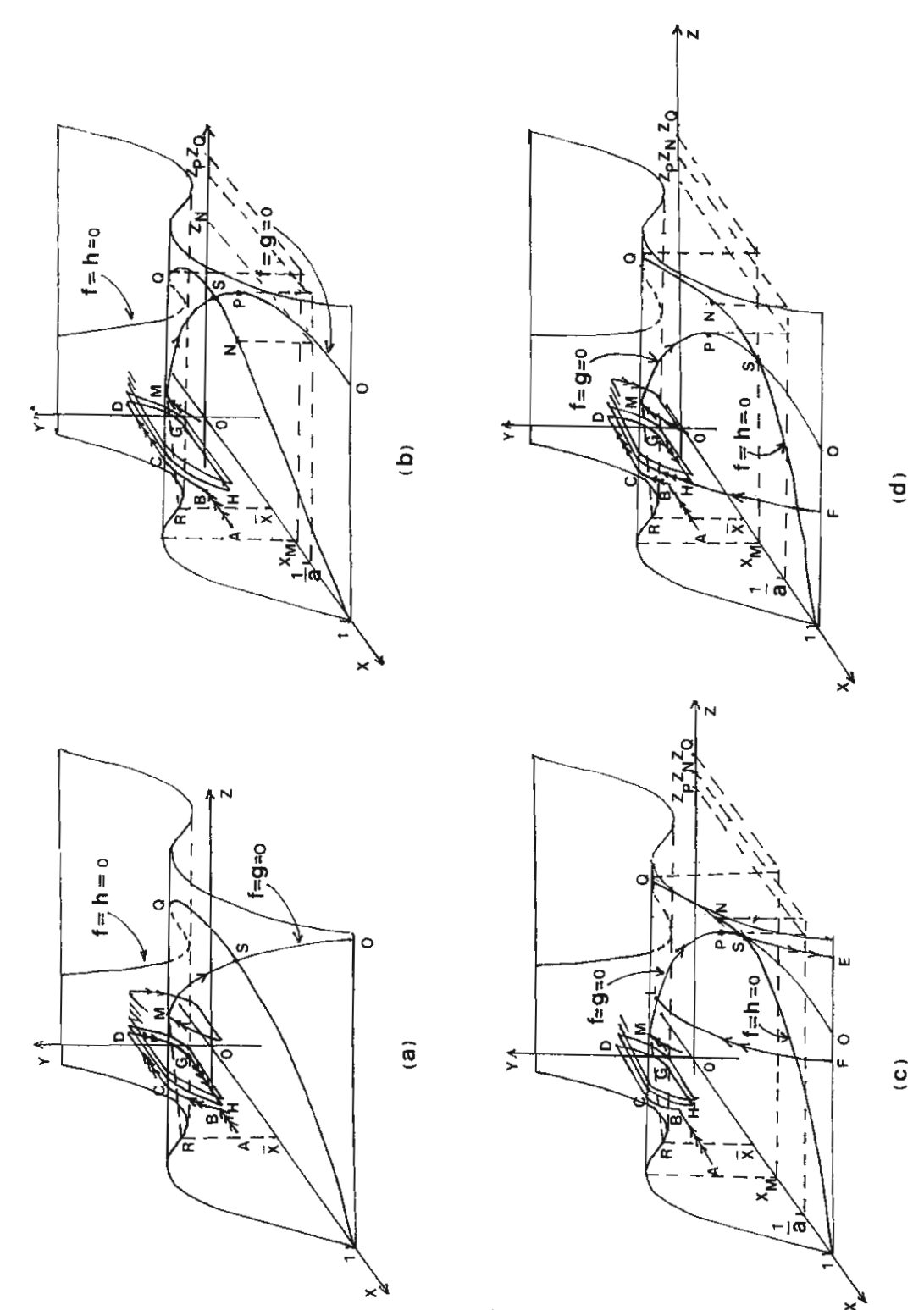


Fig. 4. Trajectories of the model system (Eqs. (9)-(11)) in Case 1 exhibiting four possible subcases 1(a), 1(b) and 1(c) identified in the text.

2.2.1.1. Case 1(a). This case is identified by the inequality

$$a < 1$$
 (33)

so that the turning point P is below the (x, z)plane corresponding to Fig. 4a in this case. Thus, starting from an initial point A in Fig. 4a, a fast transient takes us to the point B on the stable part of the fast manifold f = 0. Transition of intermediate speed is then made along this manifold in the direction of increasing y until the point C is reached where stability is lost. A fast jump is made to the point D on the other stable branch of the manifold f = 0 from which point a transition of intermediate speed develops downward until stability is lost again at the point G. A quick jump back to H almost closes up the cycle. However, z has been slowly increasing in the meantime so that the same cycling transitions are repeated in the direction of increasing z, densely covering the surface f = 0, until the point M is reached. The transient now follows the curve f = g = 0 until the point S is reached in the case I(a). In this case, the point S where $\dot{x} = \dot{y} = \dot{z} = 0$ is on the stable part of the manifold f = g = 0 and thus the transitions end at this stable equilibrium point, as shown in Fig. 4a.

2.2.1.2. Case 1(b). This is the case identified by the inequality

$$a > 1 \tag{34}$$

so that the point P is located on f = 0 above the (x, z)-plane as shown in Fig. 4b. This case is also identified by the fact that the point S, where f = g = h = 0, is located on the stable part of the curve f = g = 0. This situation is guaranteed by requiring that

$$z_{\rm p} > z_{\rm N} \tag{35}$$

where $N(x_N, y_N, z_N)$ is the point on the curve f = h = 0 with $x_N = 1/a$. From equating f and h to zero, we find that

$$z_N = \frac{\eta d_1}{\gamma d_3} \left(1 - \frac{1}{a} \right) \left(\frac{1}{a} + \beta \right) \tag{36}$$

while, from Eq. (26), we have

$$z_{p} = \frac{1}{\varepsilon} \left(\frac{\omega}{aed_{2}} - 1 \right) \tag{37}$$

Therefore, so that S is located on the stable part of f = g = 0, we require

$$\frac{\omega}{d_2} > ae \left[\frac{\epsilon \eta d_1}{\gamma d_3} \left(1 - \frac{1}{a} \right) \left(\frac{1}{a} + \beta \right) + 1 \right]$$
 (38)

which guarantees that Eq. (35) holds.

In this case 1(b) then, the transition in Fig. 4b also reaches the point S first and ends there since it is a stable equilibrium point where $\dot{x} = \dot{y} = \dot{z} = 0$. Moreover, along the curve f = h = 0 we have

$$z = \frac{\eta d_1}{\gamma d_3}$$

when x = 0. Therefore we must also require that

$$\frac{\eta d_1 \beta}{\gamma d_3} > \frac{1}{ae} \tag{39}$$

to ensure that the curve f = h = 0 intersects the curve f = g = 0 only once.

2.2.1.3. Case 1(c). This case is identified by Eq. (34) and the opposite inequality to Eq. (38), that is

$$\frac{\omega}{d_2} < ae \left[\frac{\varepsilon \eta d_1}{\gamma d_3} \left(1 - \frac{1}{a} \right) \left(\frac{1}{a} + \beta \right) + 1 \right] \tag{40}$$

which guarantees that the point P is reached first during the transition from the point M in Fig. 4c. At the point P, there is a loss of stability and a quick jump to F takes place. A slow transition develops now along this manifold where x = 1 until a point is reached where stability is again lost at some point F. A transition of intermediate speed will develop along the fast manifold f = 0 back to the point F then the same path to F is followed which completes the limit cycle in the case F 1(c).

2.2.1.4. Case l(d). In order that the transition goes back into high-frequency oscillations in each low-frequency cycle, we need to require that $z_O < z_M$, which is equivalent to

$$e^{-a} < \frac{1-\beta}{2} e^{-a(1-\beta)/2}$$
 (41)

Thus, starting from the point A in Fig. 4d, a fast transition takes us, as explained earlier, to the point B on f = 0. An intermediate transition develops on this manifold until C is reached where the stability of the equilibrium fast manifold is lost. A fast transition then takes the system to the stable equilibrium point D. An intermediate speed transition is then made along this branch of manifold until G is reached where the stability is again lost and a quick jump brings us to the stable point H. This almost closes up the cycle but just misses the point B. The slow system has becomes active and z has been slowly increasing since $\dot{z} > 0$ here. Transitions then develop following the same pattern but with slowly varying z as seen in Fig. 4d until M is reached, at which point the trajectory develops into a slow cycle which goes back into the fast cycles since Eq. (41) guarantees that z_O z_M .

2.2.2. Case 2

We observe that in this case the point R is located on the stable part of the fast manifold f = 0 as shown in Fig. 5. Mainly three subcases can therefore be identified here.

2.2.2.1. Case 2(a). If Eq. (21) as well as Eq. (33) hold then starting from the point A in Fig. 5a, a fast transition develops to the point B, followed by a transient of intermediate speed to C, from which point a slow transient takes us to the stable equilibrium point S where the transition ends.

2.2.2.2. Case 2(b). If Eq. (21) holds as well as Eq. (38) then, similarly to Case 2(a), transients in Fig. 5b develop toward the stable equilibrium point S where $\dot{x} = \dot{y} = \dot{z} = 0$ and the transition ends.

2.2.2.3. Case 2(c). Finally, if Eq. (21) holds as well as Eq. (40) then, from the point C in Fig. 5c, the point P is reached first where the stability is lost. A quick jump to E, followed by a transition at slow speed from E to F, then at intermediate speed back to E, closes the trajectory up into a low-frequency limit cycle for this case E(c).

The above analysis can be summarized by the following theorem.

2.2.3. Theorem

If ε and δ are sufficiently small, and if Eqs. (16), (30) and (32) and Eq. (39) hold, then the system Eqs. (9)–(11) has a global attractor which is a stable equilibrium if Eq. (18) and Eq. (33) hold, or Eqs. (18) and (34) and Eq. (38) hold, or if Eq. (21) and Eq. (33) or Eq. (38) hold. On the other hand, the attractor will be a low-frequency limit cycle if Eq. (21) and Eq. (40) hold, or if Eqs. (18) and (34) and Eq. (40) hold. Moreover, the low-frequency limit cycle will contain a period of high frequency oscillations if inequalities Eqs. (18), (34) and (40) and Eq. (41) hold as well.

3. Numerical results and discussion

Fig. 6a shows a numerical simulation of the model Eqs. (9)-(11) with parametric values chosen to satisfy inequalities Eqs. (18), (30), (32), (34) and (39) and Eq. (40). This is therefore the case 1(c) and the solution trajectory develops into a low-frequency limit cycle as predicted. The corresponding time courses of the three variables are shown in Fig. 7a. Fig. 6b shows a numerical simulation of the model Eqs. (9)-(11) with parametric values chosen to satisfy inequalities Eqs. (18), (30), (32), (34), (39) and (40) as well as Eq. (41). This is therefore the case 1(d). The solution trajectory develops into a low-frequency limit cycle which contains high frequency oscillations as predicted in the above theorem. The corresponding time courses of the three variables are shown in Fig. 7b. Such underlying high frequency cycles during a low frequency cycle in the biomass concentration profile have frequently been observed by a number of investigators (Chen and McDonald, 1990a,b). In Chen and McDonald, 1990b, the total budding cells count in their bioreactor data shows oscillatory behavior closely resembling our result of case 1(d) shown in Fig. 7b. Experimenting with different values for the system parameters such as β , d_3 , a, and so on, shows that the frequencies and amplitude of oscillations can be appropriately adjusted to fit different chemostat conditions.

We observe that the constant a plays an important role in the kinetics of the chemostat under

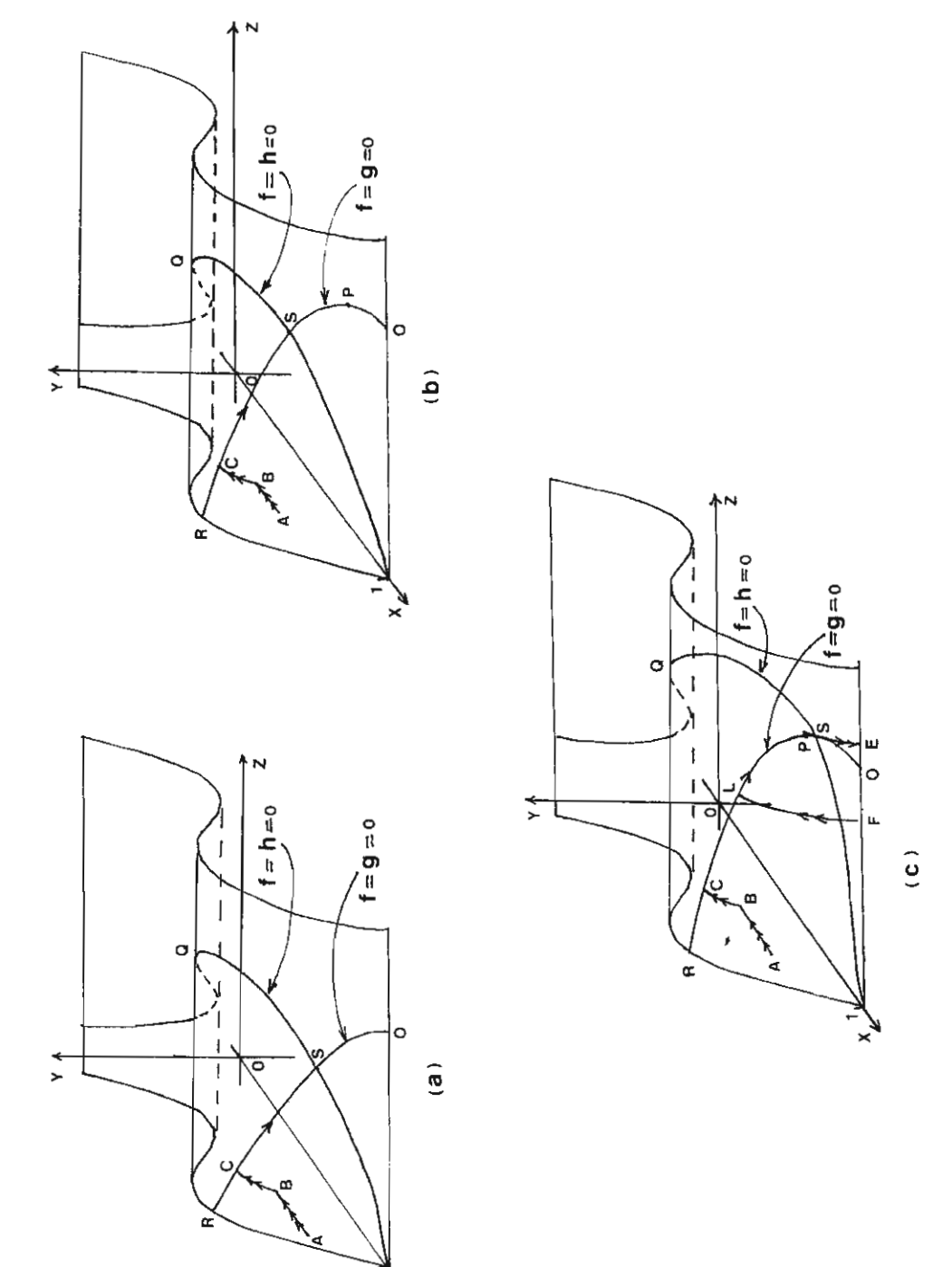


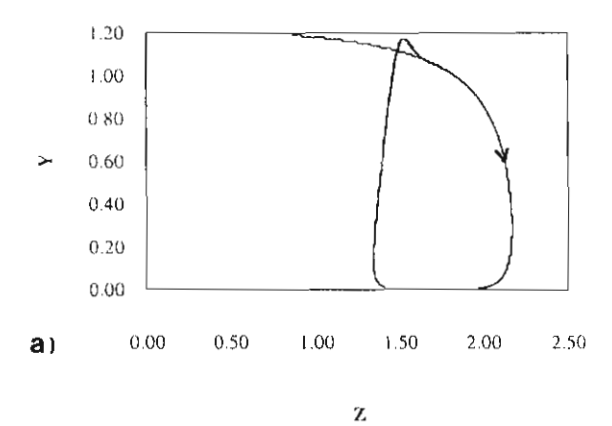
Fig. 5. Trajectories of the model system (Eqs. (9)-(11)) in Case 2 exhibiting three possible subcases 2(a), 2(b) and 2(c) identified in the text.

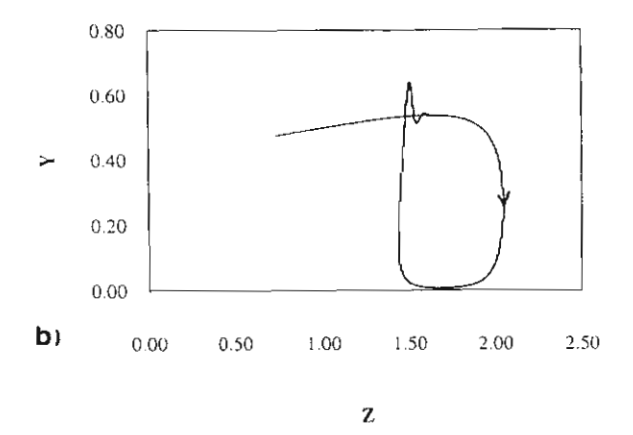
study. Considering the model in Eq. (7), a is in fact an indicator of how late or how soon the substrate inhibition sets in. In Fig. 1, substrate inhibition seems to set in approximately half way to the maximum substrate level, suggesting that a should by around 2. Thus, the numerical results presented in Fig. 6a, b can be considered as corresponding to the case where substrate inhibition is late in setting in (a < 2). In Fig. 6c, we present a numerical simulation of Eqs. (9)-(11) in which a = 2.5, thus corresponding to the situation where the inhibition sets in rather early (a > 2). With this value of a, Eq. (32) is violated and $z_0 < 0$. Therefore, the transition develops from the point E (in Fig. 4c or Fig. 5c) all the way to the point (1, 0, 0) on the x-axis which is a stable washout steady state of the system. Fig. 7c shows the corresponding time courses of the state variables in this case, where both the cells and product levels are seen to decrease toward zero, while the substrate level tends toward the maximum level $(S = S_F)$.

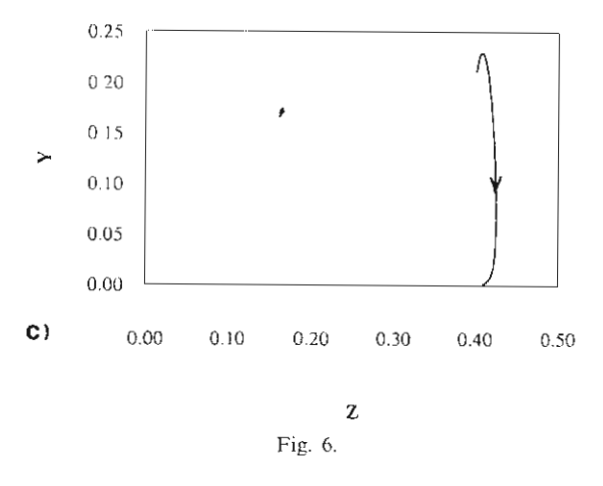
Also, it is numerically found that solution trajectories can still develop as theoretically predicted even though the values of ε and δ are not so small, and the assumption that the three components of the system carry highly diversified dynamics can be relaxed to a certain extent.

4. Conclusion

The appearance of sustained oscillations in bioreactor variables in continuous cultures indicates the complex nature of microbial systems, and the difficulties which may arise in bioprocess control and optimization.







In this paper, the dynamic behavior of a continuous bioreactor described by Eqs. (9)–(11) has been investigated, incorporating the inhibitory ef-

Fig. 6. Numerical simulation of the model equations (Eqs. (9) (11)). Here, $\varepsilon = 0.1$, $\delta = 0.01$, $\gamma = 2.0$, $\eta = 10.0$, $\omega = 3.0$, $d_1 = 0.25$, $d_2 = 0.25$, and $d_3 = 0.1$. In 6(a), the parametric values satisfy the inequalities of Case 1(c), with $\beta = 0.8$, a = 1.5, and the solution trajectory tends toward a low-frequency limit cycle as theoretically predicted. In 6(b), the parametric values satisfy the inequalities of Case 1(d), with $\beta = 0.2$, a = 1.5, and the solution trajectory tends toward a low-frequency limit cycle which contains a period of high-frequency oscillations. In 6(c), $\beta = 0.2$, and a = 2.5 which corresponds to the situation where substrate inhibition is early in setting in.

C)

Fig. 7. The time courses of the state variables x(t), y(t) and z(t) are shown here corresponding to the three respective cases seen in Fig. 6. , Represents x(t) + 2.2 in 7(a), x(t) + 0.4 in 7(b), and x(t) in 7(c). $\bigcirc - \bigcirc$, Represents y(t). x - x, Represents z(t) + 0.3 in 7(a), and z(t) in 7(b) and 7(c).

300

400

500

200

100

fect at high levels of product and substrate concentrations. Assuming that the time responses of the three components are highly diversified, increasing from bottom to top, we were able to use standard singular perturbation analysis to describe the nature of the transients and the attractors of the system.

Complex oscillatory behavior is extremely undesirable not only for general control and design problems, but also because of the possible potential for dangerous situations which may arise where toxic compounds are involved, such as in the operation of toxic waste treatment processes. Insights that can be gained from this type of analysis described above should prove most valuable in the light of such considerations.

Acknowledgements

Appreciation is expressed to the Thailand Research Fund for the financial support which made this research project possible.

Appendix A. Nomenclature

- X concentration of cells in bioreactor, g/l
- S concentration of substrate in bioreactor, g/
- S_F concentration of substrate in the feeding solution, g/l
- P concentration of product in biorector, g/l
- T time (h),
- K positive constants, g/l
- D dilution rate (h 1)
- Y yield coefficient, g cell/g substrate
- μ specific growth rate (h⁻¹)
- $\mu_{\rm m}$ maximum specific growth rate (h⁻¹)

References

Agrawal, P., Lee, C., Lim, H.C., Ramkrishna, D., 1982. Theoretical investigations of dynamic behavior of isothermal continuous stirred tank biological reactors. Chem. Eng. Sci. 37 (3), 453-462.

- Aiba, S., Shoda, M., 1969. Reassesment of the product inhibition of alcohol fermentation. J. Ferment. Technol. 47, 790–799.
- Andrews, J.F., 1968. A mathematical model for the continuous culture of microorgnisms utilizing inhibitory substrates. Biotechnol. Bioeng. 10, 707-723.
- Bazua, C.D., Wilke, C.R., 1977. Ethanol effects on the kinetics of a continuous fermentation with Saccharomyces cerevisiae. Biotechnol. Bioeng. Symp. 7, 105–118.
- Chen, C.-I., McDonald, K.A., 1990a. Oscillatory behavior of Saccharomyces cerevisiae in continuous culture: I effects of pH and nitrogen levels. Biotechnol. Bioeng. 36, 19–27.
- Chen, C.-I., McDonald, K.A., 1990b. Oscillatory behavior of Saccharomyces cerevisiae in continuous culture: II analysis of cell synchronization and metabolism, Biotechnol. Bioeng. 36, 28-38.
- Hoppensteadt, F., 1974. Asymptotic stability in singular perturbation problems II: problems having matched asymptotic expansions, J. Differ. Equ. 15, 510 512.
- Lenbury, Y., Novaprateep, B., Wiwaipataphee, B., 1994. Dynamic behavior classification of a model for a continuous bio-reactor subject to product inhibition. Math. Comput. Modelling 19 (12), 107—117.

- Monod, J., 1942. Recherces pur la crocssance des cultures bacteriennes. Hermann et Cie, Paris.
- Muratori, S., Rinaldi, S., 1989. Remarks on competitive coexistence. Siam J. Appl. Math. 49 (5), 1462–1472.
- Muratori, S., 1991. An application of the separation principle for detecting slow-fast limit cycles in a three-dimensional system. Appl. Math. Comput. 43, 1–18.
- Muratori, S., Rinaldi, S., 1992. Low- and high-frequency oscillations in three dimensional food chain systems. Siam J. Appl. Math. 52 (6), 1688–1706.
- Ramkrishna, D., Fredrickson, A.G., Tsuchiya, H.M., 1967.
 Dynamics of microbial propagation: models considering inhibitors and variable cell composition. Biotech. Bioeng. 9, 129–170.
- Thatipamala, R., Rohani, S., Hill, G.A., 1992. Effects of high product and substrate inhibitions on the kinetics and biomass and product yields during ethanol batch fermentation. Biotechnol. Bioeng. 40, 289–297.
- Yano, T., Koga, S., 1969. Dynamic behavior of the chemostat subject to substrate inhibition. Biotechnol. Bioeng. 11, 139-153.
- Yano, T., Koga, S., 1973. Dynamic behavior of the chemostat subject to product inhibition. J. Gen. Appl. Microbiol. 19, 97–114.



Mathematical and Computer Modelling

Systems Science & Mathematics Washington University, Campus Box 1040 One Brookings Drive St. Louis, Missouri 63130-4899, U.S.A. Telephone: (314) 935-6007 or 5806 Facsimile: (314) 935-6121 email: rodin@rodin.wustl.edu

An International Journal

Editor-in-Chief: Ervin Y. Rodin

Dr. Yongwimon Lenbury Department of Mathematics Faculty of Science Mahildol University Rama 6 Rd. Bangkok 10400 THAILAND

March 5, 1999

Dear Dr. Lenbury:

I am pleased to inform you that your revised paper, entitled Predator-Prey Interaction Coupled by Parasitic Infection: Limit Cycles and Chaotic Behavior MCM2853, has been accepted for publication in Mathematical and Computer Modelling. Please note the following items that are marked:

Thank you for sending the digital version of your paper, which we have received.

You may be able to reduce, by several months, the time necessary for the typesetting process if you supply a digital version of your paper. Any of these versions can be supplied on a 3.5 in, diskette or by electronic mail (publish@rodin.wustl.edu). Please supply one of the following:

- A TEX version of your paper (AMS-TEX is preferred, but LaTEX and Plain TEX are welcome).
- · A digital version of your paper. Indicate the software used, include an ascii (plain text) and a formatted version. (Please note that we are unable to make use of postscript files of the paper.)

The hard copy of your manuscript must match the file on the disk or electronic version. If you have made changes, forward a hard copy printed from the digital version. In the case of discrepancies, the hard copy will be used.

Appropriate digital files for your figures (see Manuscript Requirements enclosed) are required for publication. Original, full-sized hard copies are also necessary.

Please provide keywords (approximately 5) for your manuscript.

Complete the enclosed copyright form and return it to this office. Publication of your manuscript is subject to receipt of this completed form.

Note that we are unable to proceed with the processing of your manuscript until we hear from you on the above-mentioned matters.

For additional reprints of your article or copies of the issue in which it appears, complete the enclosed reprint order form and return it to this office. (Fifty reprints are automatically supplied free-of-charge.)

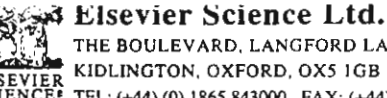
EYR:cdb

Prof. Ervin Y. Rodin

Editor in Chief

Director, Center for Optimization and Semantic Control

An Imprint of Elsevier Science Ltd



THE BOULEVARD, LANGFORD LANE, KIDLINGTON, OXFORD, OX5 1GB TEL: (+44) (0) 1865 843000 FAX: (+44) (0) 1865 843010 Expiry date Date

506 (11/96) NLG CRC EX

PREDATOR-PREY INTERACTION COUPLED BY PARASITIC INFECTION: LIMIT CYCLES AND CHAOTIC BEHAVIOR

Yongwimon Lenbury ¹
Sahattaya Rattanamongkonkul
Nardtida Tumrasvin
Somkid Amornsamankul

Department of Mathematics
Faculty of Science, Mahildol University
Rama 6 Rd., Bangkok 10400
Thailand.

email: scylb@mucc.mahidol.ac.th

¹to whom all correspondence should be addressed.

PREDATOR-PREY INTERACTION COUPLED BY PARASITIC INFECTION: LIMIT CYCLES AND CHAOTIC BEHAVIOR

Y. LENBURY, S. RATTANAMONGKONKUL N. TUMRASVIN AND S. AMORNSAMANKUL Department of Mathematics, Faculty of Science Mahildol University, Bangkok, Thailand email: scylb@mucc.mahidol.ac.th

Abstract—Several extensive studies have been carried out to document the ability of parasites to alter the behavior of infected hosts [1]-[3]. In this paper, we discuss the population dynamic consequences of parasite-induced changes in the behavior of the two interacting species in a predator-prey system, by means of the development and analysis of mathematical models. First, in order to investigate the dynamic consequences of the parasite-induced changes in the foraging ability of the predator population, a model is proposed for the predator-prey system in which only the predator population is invaded by a parasite. Thus, the predator population can be divided into two groups, namely the susceptible members and the infected ones. Analysis of the model is accomplished through a singular perturbation argument, whereby explicit conditions are derived which differentiate various dynamic behaviors and show the existence of limit cycles, explaining the oscillatory patterns often observed in field data. Parasite-induced changes in the prey's susceptibility to predation can also be modelled by a system of nonlinear differential equations [4] in which the prey population is divided into 2 classes; the susceptible members and the infectives, while the entire predator population is assumed to be infected with the parasite. Finally, a numerical investigation is carried out on the full 4-dimensional model in which both the prey and predator populations are divided each into an infected group and a susceptible one. Bifurcation diagram is constructed in order to identify the ranges of the system parametric values for which chaotic behavior can be expected.

Keywords—Parasitic infection, Predator-prey systems, Limit cycles, Chaotic behavior.

NOMENCLATURE

	1 1 0
D_x	Removal rate of susceptible prey
D_u	Removal rate of infected prey
D_y	Removal rate of susceptible predator
D_z	Removal rate of infected predator
r	Surplus death rate of susceptible prey due to competition
S	Surplus death rate of infected prey due to competition

Natural birth rate of infected prey

Natural birth rate of susceptible prev

 β Transmission rate of prey

A

B

 β' Transmission rate of predators Predator recovery rate ρ_1 Maximum predation rate of susceptible predators on susceptible prey α Maximum predation rate of infected predators on susceptible prey γ Predation rate of susceptible predators on infected prey α' γ' Maximum predator rate of infected predators on infected prey ℓ, k, k' Half saturation constants Rate of susceptible predator reproduction per unit of infected prey consumed c_0 Rate of susceptible predator reproduction per unit of susceptible prey consumed c_1 Rate of infected predator reproduction per unit of susceptible prey consumed c_2 Rate of infected predator reproduction per unit of infected prey consumed C_3 Susceptible prey population density xInfected prey population density uSusceptible predator population density y

INTRODUCTION

Infected predator population density

z

Many previous studies typically considered predation and competition to be the important factors which influence both the individual and social behavior of different animal species [3]. An accumulating body of evidence has suggested, however, that parasites (braodly defined to include viruses, bacteria, protozoans, helminths and arthropods) also play an important part in determining both the density and long-term population dynamics of many animal populations [5]-[7].

Several researchers have discovered evidence that infected hosts behave in a fashion similar to that of uninfected hosts that have either recently engaged in exhausting aerobic physical activity or have been nutritionally stressed [3]. A study by Crowden and Broom [8] of Dace infected with the parasite eye-fluke Diplostomum spathaceum, reports that infected fish develops reduced visual acuity which diminishes their ability to locate and capture their food. Other authors of several studies [9]-[10] discovered that parasitized individuals become noticeably more sluggish in their behavior as well as less gregarious and often leave the groups that afford them protection. A study of Milinski [11] also reports changes in the foraging behavior of hosts concomitantly parasitized by Schistocephalus solidus and Glugea anomale. In isopods infected with Acanthocephalus dirus and A. lucii, the parasite has been found to impair the ability of the host to use its chromatophores as an effective camouflage mechanism [12]. Thus, while uninfected hosts remain relatively inconspicuous when feeding on a similarly coloured substrate, the infected hosts are more visible which not only results in less success in thier foraging for food but also renders them more susceptible to predation and thereby increase their mortality rate.

In all cases where it has been checked for, the parasites have a negative effect on host survival, while 70 percent of the parasites were reported to reduce host fecundity [3].

To investigate the dynamic consequences of such parasite-induced changes in the predator in a predator-prey system, we analyze a mathematical model consisting of three nonlinear differential equations in which the predator population is divided into two classes, the

susceptible members and the infectives. The prey is assumed to have very fast dynamics, while the predator population has a relatively slower one. This assumption is valid in many ecological systems in which predator-prey interactions typically involve species from different trophic levels, such as the beetle Trifoleum confusum Duv. which is prey to chickens, or the sticklebacks which are susceptible to predation by birds. The susceptible predator is also assumed to have a much faster dynamics than the infectives which has deminished reproductive rate owing to their defective ability to capture their prey. Thus, the system is assumed to be characterized by highly diversified time responses, and the analysis can then be carried out using a singular perturbation approach.

A model consisting of three nonlinear differential equations has previously been proposed in [4] to study the dynamical behavior of a predator-prey system in which the entire predator population is infected with a parasite, while the prey population is divided into two classes, the susceptible members and the infectives. To model the difference in the two classes' susceptibilities to predation, different functions are used for the predator functional responses of the susceptible and infected prey populations.

It is found that invasion of a predator-prey system by a strain of parasite could cause destabilization in the form of an appearance of limit cycles. On the other hand, instability in the sense of extinction could also result if parasitic infection is removed from the system.

Finally, a full four dimensional model will be investigated, where both the predator and the prey populations are infected. Chaotic behavior is found to be possible for specific ranges of the system parameters, suggesting significant biological implications that the presence of chaotic dynamics may have for general predator-prey systems which are invaded by a strain of parasite.

MODELLING PARASITE-INDUCED CHANGE IN THE PREDATOR HOST

We consider the following system of ordinary differential equations as a model of a predator-prey system, where the predator population is divided into two groups,

$$\frac{dP}{dt} = P[B(1-rP) - D_P - \frac{\alpha S}{P+\ell} - \frac{\gamma I}{P+k}]$$
 (1)

$$\frac{dS}{dt} = \frac{c_1 \alpha SP}{P + \ell} - D_S S + \rho_1 I - \beta SI \tag{2}$$

$$\frac{dS}{dt} = \frac{c_1 \alpha SP}{P + \ell} - D_S S + \rho_1 I - \beta SI$$

$$\frac{dI}{dt} = I[\beta S - D_I + \frac{c_2 \gamma P}{P + k}]$$
(2)

where P(t), S(t), and I(t), $t \ge 0$, are the prey, susceptible predator, and infected predator population densities, respectively. B is the natural birth rate of the prey population which is assumed to be logistic, while D_P , D_S , and D_I are the removal rates of prey, susceptible predator, and infected predator, respectively. Due to the action of the parasites, the infected predator population is assumed to have a higher mortality rate such that

$$D_I > D_S \tag{4}$$

A conceptual model of this system is shown in Figure 1 where the prey population P is fed upon by both the susceptible predator S and the infected predator I. Thus, S and I exert negative effect on P.

We assume that contacts between individuals in a population occur completely randomly and therefore the rate of infection varies directly as the product of the numbers of susceptible and infected predators at any time. Hence, the infection process within the predator population can be described by the term βSI in equations (2) and (3), with ρ_1 as the recovery rate.

The predator functional responses of the prey population are assumed to be of the Holling type, namely, taking the form

$$\frac{mP}{P+K}$$

for some positive constants m and K. Owing to the action of the parasites, the infected predator's ability to locate and capture their prey is impaired, and we therefore assume that

$$\gamma < \alpha$$
 (5)

and

$$\ell < k. \tag{6}$$

In what follows, we shall consider the very frequent case of interactions between very fast and very slow (or very small and very big) components of an ecosystem. The size and the time needed for reproduction and growth of the predator population is very much greater than that of the prey population. Also, the action of the parasite can reduce host fecundity and the ability to capture its prey. The infectives therefore have a slower dynamics as compared to the susceptible members. When this hierarchical order is taken to the limit of highly diversified dynamics, the analysis of the system of equations (1)-(3) can be performed through a singular perturbation technique. This method of analysis is based on purely geometric arguments which is an extension of a known method used to study relaxation oscillations in second order systems [13]. Examples where the method was described and applied can be found in the works of Muratori and Rinaldi [14]-[15] and more recently in the work on bursting activities in the pancreatic β -cells by Lenbury et al. [16].

Thus, we scale the dynamics of the three components by means of two small dimensionless positive parameters ϵ and δ , namely; we let $x=P,\ y=S,\ z=I,\ D_x=D_P,\ a=\frac{c_1\alpha}{\epsilon},\ D_y=\frac{D_S}{\epsilon},\ \rho=\frac{\rho_1}{\epsilon},\ \beta_2=\frac{\beta}{\epsilon},\ \beta_1=\frac{\beta}{\epsilon\delta},\ D_z=\frac{D_I}{\epsilon\delta},\ \text{and}\ b=\frac{c_2}{\epsilon\delta}.$ We are led to the following system of differential equations:

$$\frac{dx}{dt} = x[B(1-rx) - D_x - \frac{\alpha y}{x+\ell} - \frac{\gamma z}{x+k}] \equiv f(x,y,z)$$
 (7)

$$\frac{dy}{dt} = \epsilon \left[\frac{ayx}{x+\ell} - D_y y + \rho z - \beta_2 yz \right] \equiv \epsilon g(x,y,z)$$
 (8)

$$\frac{dz}{dt} = \epsilon \delta z [\beta_1 y - D_z + \frac{b\gamma x}{x+k}] \equiv \epsilon \delta h(x,y,z)$$
(9)

Thus, x is the fast component, while y and z are the intermediate and slow ones, respectively.

SINGULAR PERTURBATION ANALYSIS AND LIMIT CYCLES

We now show that, for suitable values of the system parameters, the geometry of the equilibrium manifolds f(x, y, z) = 0, g(x, y, z) = 0 and h(x, y, z) = 0 of the system of equations (7)-(8) are as shown in Figure 2.

Manifold f = 0

We first observe that the manifold f(x, y, z) = 0 consists of 2 parts; the trivial manifold x = 0 and the nontrivial manifold given by the equation

$$B(1-rx) - D_x - \frac{\alpha y}{x+\ell} - \frac{\gamma z}{x+k} = 0 \tag{10}$$

Equation (10) defines a surface $y = \zeta(x, z)$ given by

$$y = \zeta(x, z) \equiv \frac{x + \ell}{\alpha} \left[B(1 - rx) - D_x - \frac{\gamma z}{x + k} \right] \tag{11}$$

which intersects the xy-plane along the parabolic curve

$$y = \frac{1}{\alpha} [-Brx^2 + (B - D_x - B\ell r)x + (B - D_x)\ell]$$
 (12)

If we let x_1 be the value of x for which $\frac{dy}{dx} = 0$ along the above curve in the xy -plane, then

$$x_1 = \frac{B - D_x - B\ell r}{2Br} \tag{13}$$

Moreover, the curve reaches the positive x-axis at the point where

$$x = x_2 \equiv \frac{B - D_x}{Br} \tag{14}$$

and intersect the y-axis at the point where

$$y = y_1 \equiv \frac{\ell}{\alpha} (B - D_x) \tag{15}$$

We observe that x_2 and y_1 will be positive if

$$B > D_x. (16)$$

Finally, the manifold intersects the z-axis at the point where x = y = 0 and

$$z = z_0 \equiv \frac{k(B - D_x)}{\gamma}$$

SINGULAR PERTURBATION ANALYSIS AND LIMIT CYCLES

We now show that, for suitable values of the system parameters, the geometry of the equilibrium manifolds f(x, y, z) = 0, g(x, y, z) = 0 and h(x, y, z) = 0 of the system of equations (7)-(8) are as shown in Figure 2.

Manifold f = 0

We first observe that the manifold f(x, y, z) = 0 consists of 2 parts; the trivial manifold x = 0 and the nontrivial manifold given by the equation

$$B(1-rx) - D_x - \frac{\alpha y}{x+\ell} - \frac{\gamma z}{x+k} = 0 \tag{10}$$

Equation (10) defines a surface $y = \zeta(x, z)$ given by

$$y = \zeta(x, z) \equiv \frac{x + \ell}{\alpha} \left[B(1 - rx) - D_x - \frac{\gamma z}{x + k} \right]$$
 (11)

which intersects the xy-plane along the parabolic curve

$$y = \frac{1}{\alpha} [-Brx^2 + (B - D_x - B\ell r)x + (B - D_x)\ell]$$
 (12)

If we let x_1 be the value of x for which $\frac{dy}{dx} = 0$ along the above curve in the xy -plane, then

$$x_1 = \frac{B - D_x - B\ell r}{2Br} \tag{13}$$

Moreover, the curve reaches the positive x-axis at the point where

$$x = x_2 \equiv \frac{B - D_x}{B_x} \tag{14}$$

and intersect the y-axis at the point where

$$y = y_1 \equiv \frac{\ell}{\alpha} (B - D_x) \tag{15}$$

We observe that x_2 and y_1 will be positive if

$$B > D_x. (16)$$

Finally, the manifold intersects the z-axis at the point where x = y = 0 and

$$z = z_0 \equiv \frac{k(B - D_x)}{\gamma}$$

Manifold g = 0

The manifold g(x, y, z) = 0 is given by the equation

$$\frac{axy}{x+\ell} - D_y y + \rho z - \beta_2 y z = 0 \tag{17}$$

which defines a surface $x = \nu(y, z)$ given by

$$x = \nu(y, z) \equiv \frac{(D_y y - \rho z + \beta_2 y z)\ell}{ay - D_y y + \rho z - \beta_2 y z}$$

$$\tag{18}$$

Letting z = 0 in (18), we find that this surface intersects the xy-plane (see Figure 2) along the line

$$x = x_3 \equiv \frac{D_y \ell}{a - D_y} \tag{19}$$

Putting x = 0 in (10) and (17), and letting

$$\theta = \alpha \rho k + \ell \gamma D_y - \beta_2 k (B - D_x) \tag{20}$$

we find that the curve f(x, y, z) = g(x, y, z) = 0 intersects the yz-plane at the point where

$$z = z_1 \equiv \frac{-\theta + \sqrt{\theta^2 + 4\gamma\ell^2kD_y\beta_2(B - D_x)}}{2\gamma\ell\beta_2}$$
 (21)

which will be positive if, again, inequality (16) holds.

Manifold h = 0

We observe that the manifold h(x, y, z) = 0 consists of 2 parts; the trivial manifold z = 0 and the nontrivial manifold given by the equation

$$y = \frac{1}{\beta_1} (D_z - \frac{b\gamma x}{x+k}) \tag{22}$$

which is parallel to the z-axis (see Figure 2).

The value of x_4 in Figure 2 is found by setting y = 0 in equation (22) and solving for x, which leads to

$$x_4 = \frac{D_z k}{b\gamma - D_z} \tag{23}$$

which will be positive provided that

$$b\gamma > D_z \tag{24}$$

Also, the manifold in (22) intersects the yz-plane along the line

$$y = y_2 \equiv \frac{D_z}{\beta_1} \tag{25}$$

Letting x = 0 and $y = y_2$ in (10) we find that the curve f(x, y, z) = h(x, y, z) = 0 intersects the yz-plane at the point where

$$z = z_2 \equiv \frac{k}{\gamma} (B - D_x - \frac{\alpha D_z}{\ell \beta_1}) \tag{26}$$

Finally, by putting $x = x_4$ and y = 0 in (10) we find that the curve f(x, y, z) = g(x, y, z) = 0 intersects the xz-plane at the point where

$$z = z_3 \equiv \frac{bk}{b\gamma - D_z} (B - D_x - \frac{BrD_z k}{b\gamma - D_z})$$
 (27)

We now identify and analyze each of the five possible cases 1 through 5 which correspond to the five subfigures 2a through 2e of Figure 2, respectively, differentiated according to the relative positions of the points x_1 through x_4 , y_1 , y_2 and z_1 through z_3 previously defined. In Figure 2a, the point x_1 is above x_3 on the positive x-axis, while the point x_4 is located between the points x_2 and x_3 . In Figure 2b, the point x_1 is below x_3 on the positive x-axis so that the transitions will develop along a different path. In Figure 2c, on the other hand, the value of x_1 , given by (13), is negative while x_3 , given by (19), is still positive. Figure 1d corresponds to the case in which the value of x_4 , given by (23), is larger than both x_2 and x_3 , and at the same time z_3 , given by (27), is now negative. The last case of Figure 2d is identified by the condition that the value of y_1 , given by (15), is extremely small so that the point y_1 is a lot closer to the origin than the point y_2 on the positive y-axis. The following 5 cases can then be identified.

Case 1 (Figure 2a) This case is identified by the inequalities

$$x_1 > 0 \tag{28}$$

$$x_1 > x_3$$
 (29)

$$x_2 > x_4 > x_3 > 0 \tag{30}$$

$$y_1 > y_2 \tag{31}$$

$$z_3 > 0 \tag{32}$$

$$z_0 > z_1 > z_2, z_1 > 0 (33)$$

which ensure that the manifolds are shaped as in Figure 2a, where transitions of slow, intermediate and high speeds are indicated by one, two, and three arrows, respectively.

For small values of ϵ and δ , the slow (z) and intermediate (y) variables are frozen at their initial values z(0) and y(0), and the evolution of the fast component of the system is determined by solving the 'fast system'

$$\dot{x}(t) = f(x(t), y(0), z(0)) \tag{34}$$

Thus, x(t) tends asymptotically to one of the stable equilibria of the fast system (in general, characterized by $\frac{\partial f}{\partial x} < 0$).

Therefore, starting from a generic point, say point A, above the nontrivial manifold f = 0, a trajectory develops at constant y and z and reaches a point B on the stable branch of the fast manifold f(x, y, z) = 0 at high speed.

Once the state of the system has reached the fast manifold f = 0, the intermediate system has now become active and is governed by

$$\dot{y}(t) = g(\bar{x}(x(0), y(t), z(0)), y(t), z(0)) \tag{35}$$

where $\bar{x}(x(0), y(t), z(0))$ is a stable equilibrium of the fast system with y(0) substituted by y.

Then, keeping z still frozen at z(0), transition develops at intermediate speed along the manifold f=0 in the direction of increasing y since g>0 here, toward the point C where the stability of the manifold is lost and a quick transition is made to the point D on the yz-plane which is stable. Since the segment DE (in Figure 2a) is below the manifold g=0 so that g<0 here, a transition at intermediate speed will be made in the direction of decreasing y from D toward E.

At the point E, the stability of the trivial manifold x=0 will be lost and a quick jump is made toward the point F which almost closes the cycle. However, since z has been slowly increasing during the transitions, F just misses the path BC. The same cycling process is now repeated with slowly increasing z, densely filling out the space until the point G is reached. Since g>0 here, a transition slowly develops along GH towards the point H, where a saddle-node bifurcation occurs. A catastrophic transition from H to K then takes place followed by a slow transition from K towards L, since the point K is in front of the manifold h(x,y,z)=0 so that h<0 and z is decreasing along this portion of the line KL. Once the point L is reached a quick jump back to G closes up the transition GHKL, resulting in a limit cycle composed of the concatenation of transitions occurring at two different speeds; namely, 2 fast and 2 slow ones.

The existence and locations of the points E and L have been discussed and proved by Schecter [17] and Osipove et al. [18]. Transients of varying speeds along these manifolds will form a path, which results in a closed cycle in this case. Such a path approximates the exact solution to the model system equations (7)-(9) in the sense that the solution trajectory will be contained in a tube around that path and the radius of the tube goes to zero along with ϵ and δ .

Case 2 (Figure 2b) Here, the inequality (29) is violated so that this case is identified by the inequalities (28), (30)-(33), and

$$x_1 < x_3$$
 (36)

The positions of the manifolds are as shown in Figure 2b where the intersection point S of the 3 manifolds f = 0, g = 0, and h = 0, namely the steady state, is located on the stable portion of the nontrivial manifold f = 0. When the transitions reach the point R on the line of intersection between the manifolds f = 0 and g = 0, a slow motion develops along this line in the direction of increasing z and the transition ends once the point S in Figure 2b is reached. Thus, the solution trajectory in this case is expected to approach this stable equilibrium point S, in which situation persistence of all three populations is attained.

Case 3 (Figure 2c) In this case, inequalities (28) and (29) are violated and we instead have

$$x_1 < 0 < x_3 \tag{37}$$

while (30)-(33) still hold. The manifolds are positioned in this case as in Figure 2c where the line segment RS is in the region where h > 0. This means that, once the state of system reaches the point R, a transition of slow speed will develop in the direction of increasing z toward the point S. We therefore have, in this case, persistence of all three populations, also.

Case 4 (Figure 2d) In this case, inequalities (30) and (32) are violated and we instead have

$$0 < x_2 < x_3 < x_4 \tag{38}$$

$$z_3 < 0 \tag{39}$$

while (28),(29),(31) and (33) still hold. The positions of the manifolds are as in Figure 2d, in which the line segment from the point T to the point $(x_2,0,0)$ is in the region where h < 0. Transitions then develop toward the point $(x_2,0,0)$ where the predator population becomes extinct while the prey tends to a constant level x_2 .

Case 5 (Figure 2e) In this last case, inequality (31) is now violated and we have

$$y_1 < y_2 \tag{40}$$

and

$$y_1 << 1 \tag{41}$$

while (28)-(30), and (32) still hold. The manifolds are positioned as shown in Figure 2e. Here, along OQ we have h < 0, and once the state of the system reaches the point Q, a transition at intermediate speed will develop in the direction of decreasing z from the point Q towards the point O. Thus, in this case we have extinction of all three populations in the system.

The above analysis can be summerized as in the following theorem.

Theorem 1 If ϵ and δ are sufficiently small, the system of equations (7)-(9) possesses a positive attractor which is a stable nonwashout equilibrium state provided that inequalities (28),(30)-(33) and (36) hold, or if inequalities (30)-(33) and (37) hold. However, if inequalities (28)-(33) hold then the attractor will be a limit cycle composed of a concatenation of transitions occurring at 2 different speeds.

Figure 3 shows a computer simulation of equations (7)-(9) with parametric values chosen to satisfy the inequalities in each specific cases 1 through 5 identified above corresponding to Figures 2a to 2e, respectively. The solution trajectories are here projected onto the (z, x)-plane. The time courses of the state variable y(t) in the five cases are correspondingly presented in Figure 4.

DYNAMIC CONSEQUENCES OF INFECTION OF BOTH SPECIES

We now investigate the global dynamical behavior of the predator-prey system in which both species are infected by parasites. By letting

x =susceptible prey population density

y =susceptible predator population density

z = infected predator population density

u = infected prey population density

a conceptual model of such a system is presented in Figure 5 where the susceptible prey x and the infected prey u are fed upon by both the susceptible and infected predators. Thus, x and u exert positive effects on y and z, while both y and z have negative effects on x and u.

We therefore consider as our model the following system

$$\frac{dx}{dt} = x[B(1-rx) - \beta' - \frac{\alpha y}{x+\ell} - \frac{\gamma z}{x+k} - D_x]$$
 (42)

$$\frac{dx}{dt} = x[B(1-rx) - \beta' - \frac{\alpha y}{x+\ell} - \frac{\gamma z}{x+k} - D_x]$$

$$\frac{dy}{dt} = -\beta yz + c_0 \alpha' uy + \frac{c_1 \alpha xy}{x+\ell} - D_y y + \rho_1 z$$
(42)

$$\frac{dz}{dt} = \beta yz + \frac{c_2 \gamma xz}{x+k} + \frac{c_3 \gamma' uz}{x+k'} - D_z z \tag{44}$$

$$\frac{du}{dt} = u[A(1-su) - \alpha'y - \frac{\gamma'z}{u+k'} - D_u] + \beta'x \tag{45}$$

where the prey is logistic, with A, B, r and s being positive constants. β' is the prey transmission rate, β the predator transmission rate, D_u , D_x , D_y and D_z the removal rates of susceptible prey, infected prey, susceptible predator and infected predator, respectively.

Following the work of Lenbury [4], the predator functional response of the infected prey is given by the term $\alpha'uy$ in equations (43) and (44), while the other predator functional responses are all of the Holling type, with α' , γ' , k', α , γ , k, c_0 , c_1 , c_2 , and c_3 being positive constants. Thus, the infected prey has an increasingly higher functional response than the uninfected prey, while ρ_1 is the predator recovery rate.

In order to carry out our numerical investigation to determine the ranges of parametric values where chaotic dynamics were likely, our choice of parameters was guided by two factors. First, we still concentrate on ecological systems which are characterized by highly diversified dynamics. Accordingly, we chose parameters so that the time response of the system of equations (42)-(45) decreases from top to bottom. Second, to take into account the parasite- induced changes in the infected members, we chose

$$k > \ell$$

and

$$\alpha > \gamma$$

Furthermore, as has been noted by previous researchers [19], one may be able to generate chaos in a nonlinear system which already exhibits limit cycle behavior. We therefore chose parametric values that would lead to cycling in the x, y and z components, with u missing, guided by our work in the previous section and in [4].

Our investigation involves letting the system run for 60,000 time steps, and examining only the last 40,000 time steps to eliminate transient behavior. We used values of γ between 0.3 and 0.6, changing γ in steps of 0.001. The relative maximum values y_{max} of y, collected during the last 40,000 time steps, are plotted as a function of γ as shown in Figure 6.

We discover in this bifurcation diagram the appearance of a period doubling route to chaos, similar to those exhibited by one-dimensional difference equations such as the logistic model. Evidently, the system of equations (42)-(45) exhibits chaotic dynamics for values of γ between 0.38 and 0.43.

Finally, Figure 7 shows the solution trajectory of the model system (42)-(45) and the corresponding time series of y(t) for $\gamma = 0.43$ in the chaotic range identified in the bifurcation diagram.

ECOLOGICAL IMPLICATIONS

Our analysis of the model where only the predator population is invaded by a parasite has shown that as many as 5 qualitatively different phase portraits are possible for various suitably chosen values of the system parameters.

We observe that in Case 1, the action of parasite renders ℓ small as compared to a. The value of x_3 given by (19) is therefore smaller than x_1 , a condition which destabilizes the system and allows the limit cycles to appear.

Moreover, Case 4 is characterized by inequality (38) which is satisfied if ℓ is small enough and k is sufficiently high. The value of x_3 given by (19), is then smaller than x_4 , given by (23). Also, infection induces very high mortality rate D_z in the infected members of the predator population which renders z_3 , given by (27), smaller than zero satisfying inequality (39). This is thus the case where the action of parasitic infection is severe so that the predators become extinct while the prey persists.

In Case 5, on the other hand, the predators cannot survive, even with a low rate of parasitic infection (β_1 being very small). Without the benefit of parasitic infection, the predator's ability to capture its prey will be little impaired and $\frac{\ell}{\alpha}$ is accordingly very small. This case is thus characterized by inequalities (40)-(41) in which $y_1 < y_2$ and y_1 is very small. Predation can therefore drastically reduce the number of prey in the system, since the beneficiary effect of the parasite is absent. Therefore, the prey population can become extinct. The lack of prey then leads to the eventual extinction of the predators. Thus, in this case we have extinction of both species.

Our study clearly indicates that the presence of parasites is important for the coexistence of both species in a predator-prey system. If the infection rate is too low or too high, the system can be destabilized and extinction of one or both species may be possible. However, volumenous information exists, such as on protozoa-bacteria systems, where parasitic infection is completely absent, which tells us that these predators and prey can coexist. Specifically, the predators do not eliminate their prey even when they were free of parasitic infections. Studies also showed that a predator can eliminate its prey in certain

situations, for example in the case where an alternative prey is available to the predator and the primary prey is not growing to compensate its loss due to predation.

Therefore, in order that a more conclusive evidence can be obtained in support of our hypothesis about the crucial role of parasitic infections to predator-prey coexistence, the effects of parasites need to be incorporated into a model based upon all the other factors that contribute to the coexistence of predator and prey species. It is hoped that the present study may serve as a building block for more intensive investigations in the future to test such an important hypothesis concerning the role of parasitic infection on coexistence.

Furthermore, we have adopted, in this paper, the simplifying assumption that a parasite can infect the entire population at any given time. In reality, an infected prey or predator may be the same as an uninfected species and infection might not manifest itself until a certain period of time. Appropriate delay terms could be added to the model equations in order to incorporate such effects.

However, our study has shown that chaos is possible even for a relatively simple predatorprey model when coupled by parasitic infection. It appears that chaotic behavior may be
much more common in natural systems than what previous studies seem to have suggested.
The invasion of the parasites acts as a coupling factor which links two predator-prey subsystems, operating at markedly different time scales. One of the subsystems may oscillate
at one frequency of oscillation while the other subsystem also oscillates at other frequencies, giving rise to a very complex situation. Such chaotic dynamics are characterized by
a sentivity to initial conditions and a small change in the initial condition may result in
a completely different solution trajectory. Thus, even a slight perturbation in the species
population density, as could occur naturally, may readily lead to unpredictable outcome
through time.

CONCLUSION

In this paper, the dynamic consequences of behavioural changes in the host predator in a predator-prey system is modelled by a system of three nonlinear ordinary differential equations. Singular perturbation arguments have been used to detect limit cycle behavior as well as describe other dynamical situations which may be observed in the predator-prey interaction mediated by the action of a parasite.

The analysis of our 3-dimensional model indicates that the presence of a parasite can cause destabilization and the appearance of limit cycles (Case 1). In the near absence of the parasites ($\beta << 1$) active foraging by the predator can wipe out the prey population which leads to eventual extinction of both species in the system (Case 5). Thus, our model illustrates how parasitic infection can play a most important role in determining the density and long-term population dynamics of many animal populations. In fact, a simple predator-prey system can exhibit quite a complex dynamical behavior when mediated by the action of a parasite as our investigation of the full four dimensional model where both species are infected illustrates.

It is evident from this work that further intensive studies of the influence of parasites on their hosts' behavior, the costs and long-term evolutionary benefits of changing the influence of the parasites, as well as the mechanisms involved, should yield most valuable insights into how subtle manipulations of the host's physiology and population dynamics could be accomplished. Such discovery would have very far-reaching ecological implications indeed.

ACKNOWLEDGEMENT

Appreciation is rendered to the Thailand Research Fund and the National Research Council of Thailand for the financial support which has made possible this research project.

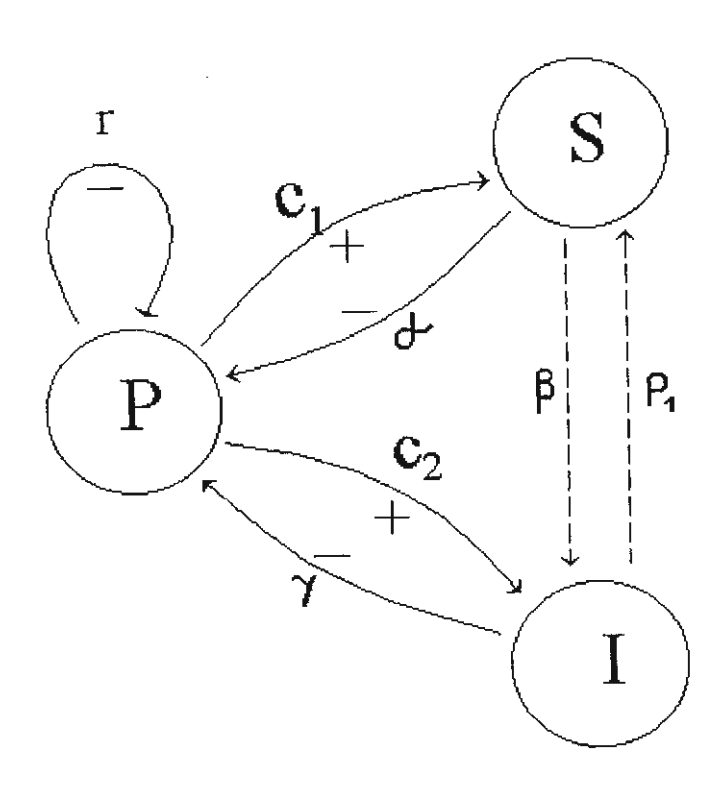
References

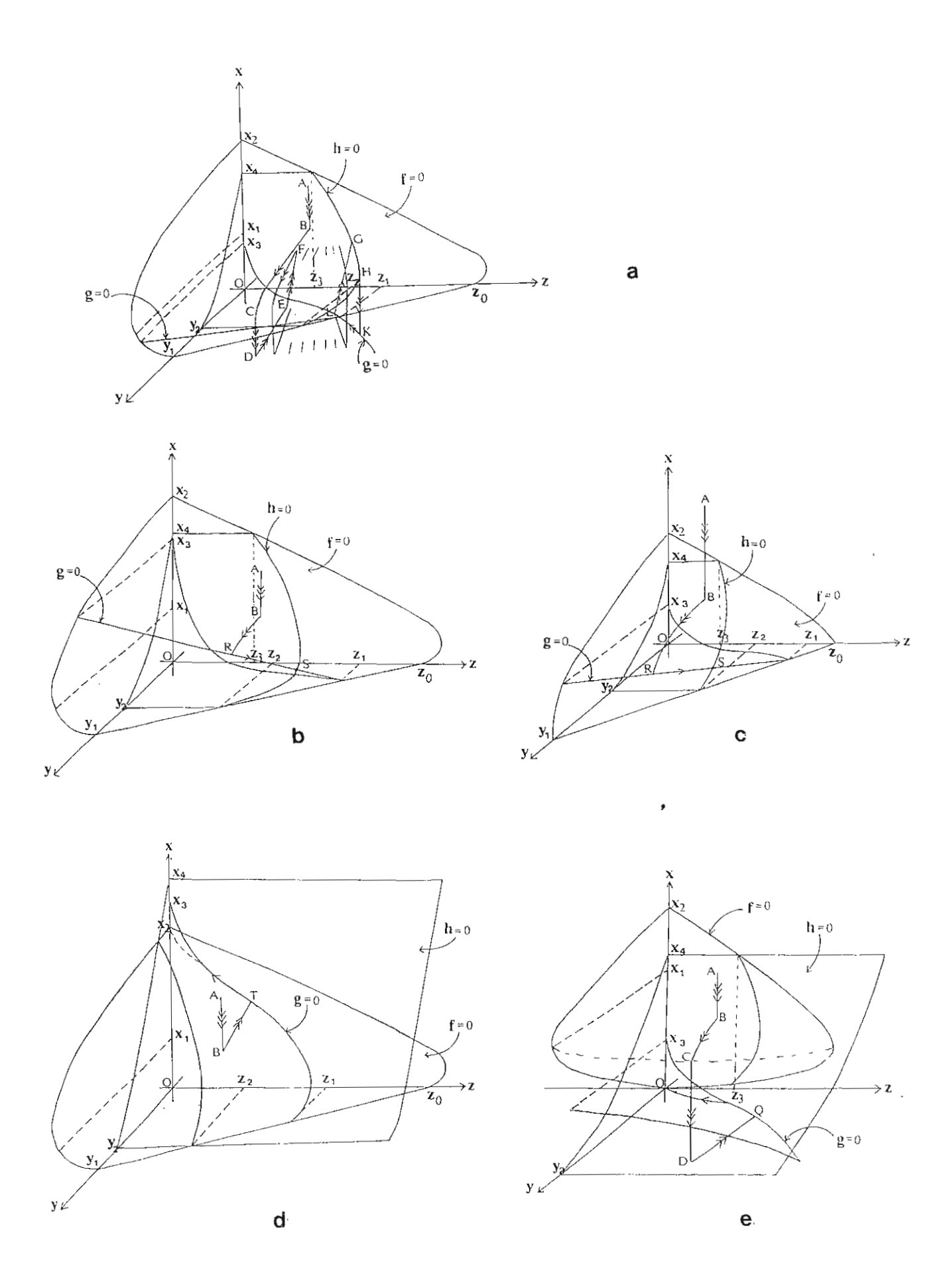
- [1] J.C.Holmes and W.M. Bethel, Modification of intermediate host behaviour by parasites. In E.U. Channing and C.A. Write (eds.). Behavioural Aspects of Parasite Transmission. Zoological Journal of the Linnean Society. Suppl. 1, 123-149 (1972).
- [2] J. Moore, Responses of an avian predator and its isopod prey to an acanthocephalan parasite. *Ecology* **64**, 1000-1015 (1983).
- [3] A.P. Dobson, The population biology of parasite-induced changes in host behavior. *Quart. Rev. Bio.* **63(2)**, 139-165 (1988).
- [4] Y. Lenbury, Singular perturbation analysis of a model for a predator-prey system invaded by a parasite. *BioSystem.* **39**, 21-262 (1996).
- [5] R.M. Anderson and R.M. May, Convolution of hosts and parasites. *Parasitol.* **85**, 411-426 (1982).
- [6] R.M. Anderson and R.M. May, The invasion, persistence and spread of infectious diseases within animal and plant communities. *Proc. Roy. Soc. Lond. B.* 314, 533-570 (1986).
- [7] R.M. Anderson and R.M. May, Spatial heterogeneity and the design of immunization programs. *Math. Biosci.* **72**, 83-111 (1979).
- [8] A.E. Crowden, and D.M. Broom, Effects of the eyefluke, *Diplostomum spathaceum*, on the behavior of dace (*Leuciscus leuciscus*). *Anim. Behav.* **28**, 287-294 (1980).
- [9] W.A. Dence, Studies on Ligula-infected common shiners (*Notropis cornutus* Agassiz) in the Adirondacks. J. Parasitol. 44, 334-338 (1958).
- [10] T.S.C. Orr, Spawning behaviour of rudd, Scardinius erythrophthalmus infected with plerocercoids of Ligula intestinalis. Nature 212, 736 (1966).
- [11] M. Milinski, Parasites determine a predator's optimal feeding strategy. Behav. Ecol. Sociobiol. 15, 35-37 (1984).
- [12] J. Brattey, The effects of the larval Acantocephalus lucii on the pigmentation, reproduction, and suscepitibility to predation of the isopod Asellus aquaticus. J. Parasitol. 69, 1172-1173 (1983).
- [13] F. Hoppensteadt, Asymptotic stability in singular perturbation problems II: problems having matched asymptotic expansions. J. Diff. Equations 15, 510-521 (1974).
- [14] S. Muratori, An application of the separation principle for detecting slow-fast limit cycles in a three-dimensional systems. *Appl. Math. Comput.* **43**, 1-18 (1991).
- [15] S. Muratori and S. Rinaldi, Low- and high-frequency oscillations in three-dimensional food chain systems. SIAM J. Appl. Math. 52(6), 1688-1706 (1992).

- [16] Y. Lenbury, K. Kumnungkit and B. Novaprateep, Detection of slow-fast limit cycles in a model for electrical activity in the pancreatic β -cells. *IMA J. Math. Appl. Med. Biol.* 13, 1-21 (1996).
- [17] S. Schecter, Persistence of unstable equilibria and closed orbits of a singularly perturbed equation. J. Diff. Equations 60, 131-141 (1985).
- [18] A.V. Osipov, G. Soderbacka, and T. Eirold, On the existence of positive periodic solutions in a dynamical system of two predator-one prey type. Viniti Deponent n 4305-B86 (Russian) (1986).
- [19] A. Hastings and T. Powell, Chaos in a three-species food chain. *Ecology* **72(3)**, 896-903 (1991).

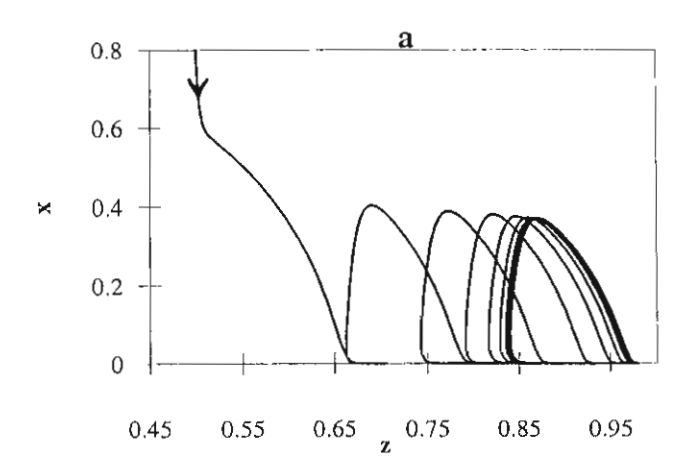
FIGURE CAPTIONS

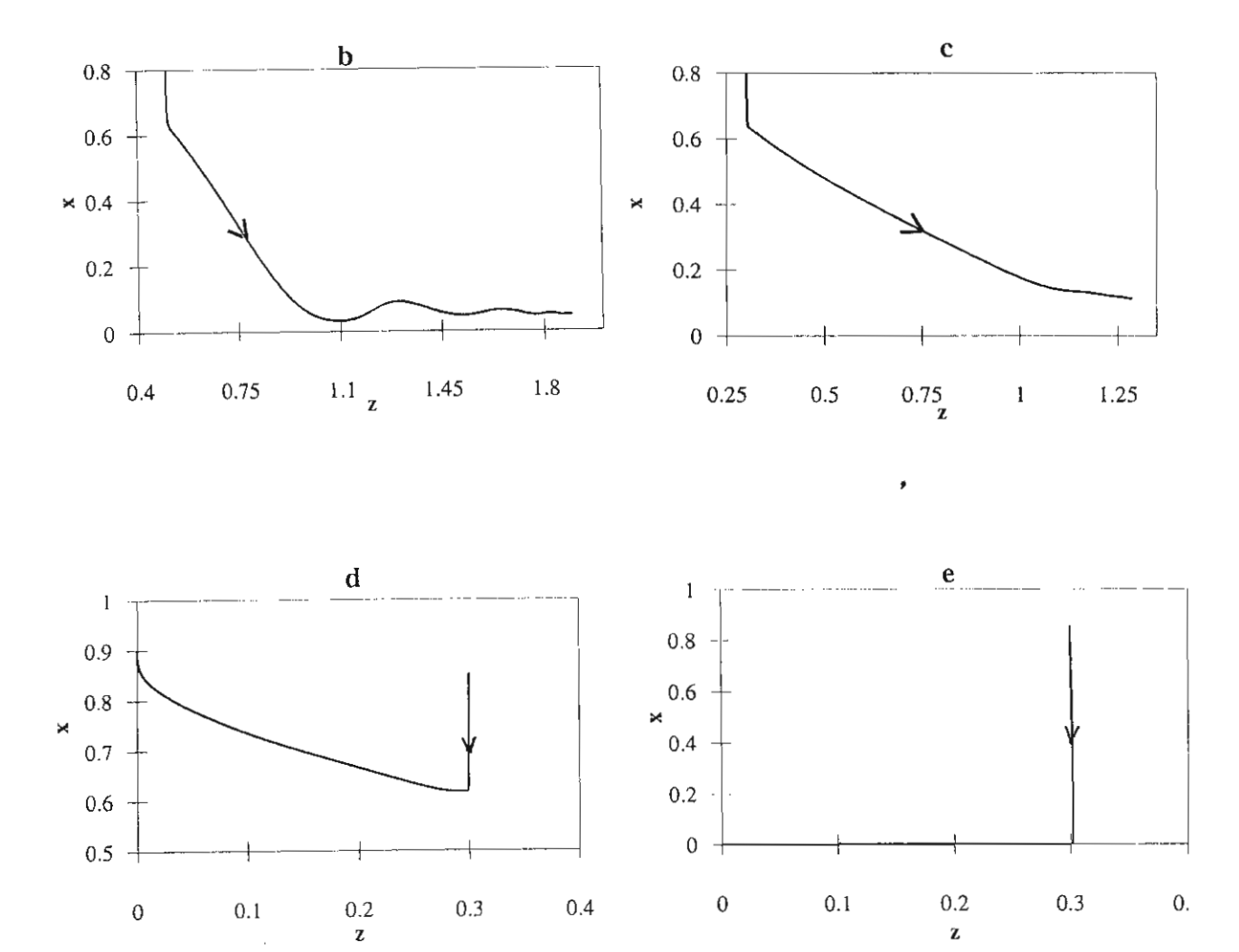
- Figure 1. Conceptual model of the predator-prey system in which only the predator population is infected.
- Figure 2. Five possible cases of trajectory development on the equilibrium manifolds for the system (7)-(9), where transitions of slow, intermediate, and high speeds are indicated by one, two, and three arrows, respectively.
- Figure 3. Computer simulation of the model system (7)-(9). The solution trajectories in subfigures 3a through 3e, corresponding to the cases 1 through 5 identified in the text, are shown projected onto the (z,x)-plane. Here, $\rho=0.07$, r=1, $\beta_1=1.0$, $\beta_2=0.1$, $\epsilon=\delta=0.1$, while a) B=3.0, a=1.0, b=4.0, $D_x=0.6$, $D_y=0.03$, $D_z=0.8$, k=0.6, $\ell=0.4$, $\ell=0.8$, $\ell=0.7$ b) $\ell=0.7$ b) $\ell=0.7$ c) $\ell=0.7$ c) $\ell=0.8$, $\ell=0.8$,
- Figure 4. The time courses of y(t) in the 5 cases corresponding to Figure 3a through 3e in Figure 3.
- Figure 5. Conceptual model of the predator-prey system in which both the predators and prey are infected.
- Figure 6. Bifurcation diagram for the model system (42)-(45) where $A=0.003,\ B=3,$ $\beta=1.0,\ \beta'=0.01,\ r=1.0,\ s=5.0,\ \alpha=0.8,\ \alpha'=0.0001,\ \gamma'=0.1,\ c_0=0.07,$ $c_1=0.125,\ c_2=0.052,\ c_3=0.7,\ \rho_1=0.7,\ k=0.3,\ k'=0.6,\ \ell=0.185,$ $D_u=0.001,\ D_x=0.001,\ D_y=0.08,\ \text{and}\ D_z=0.007.$ The plot is of the relative maximum values of y vs γ .
- Figure 7. Chaotic dynamics for the model system (42)-(45) for the parametric values of Figure 6 with $\gamma = 0.43$.

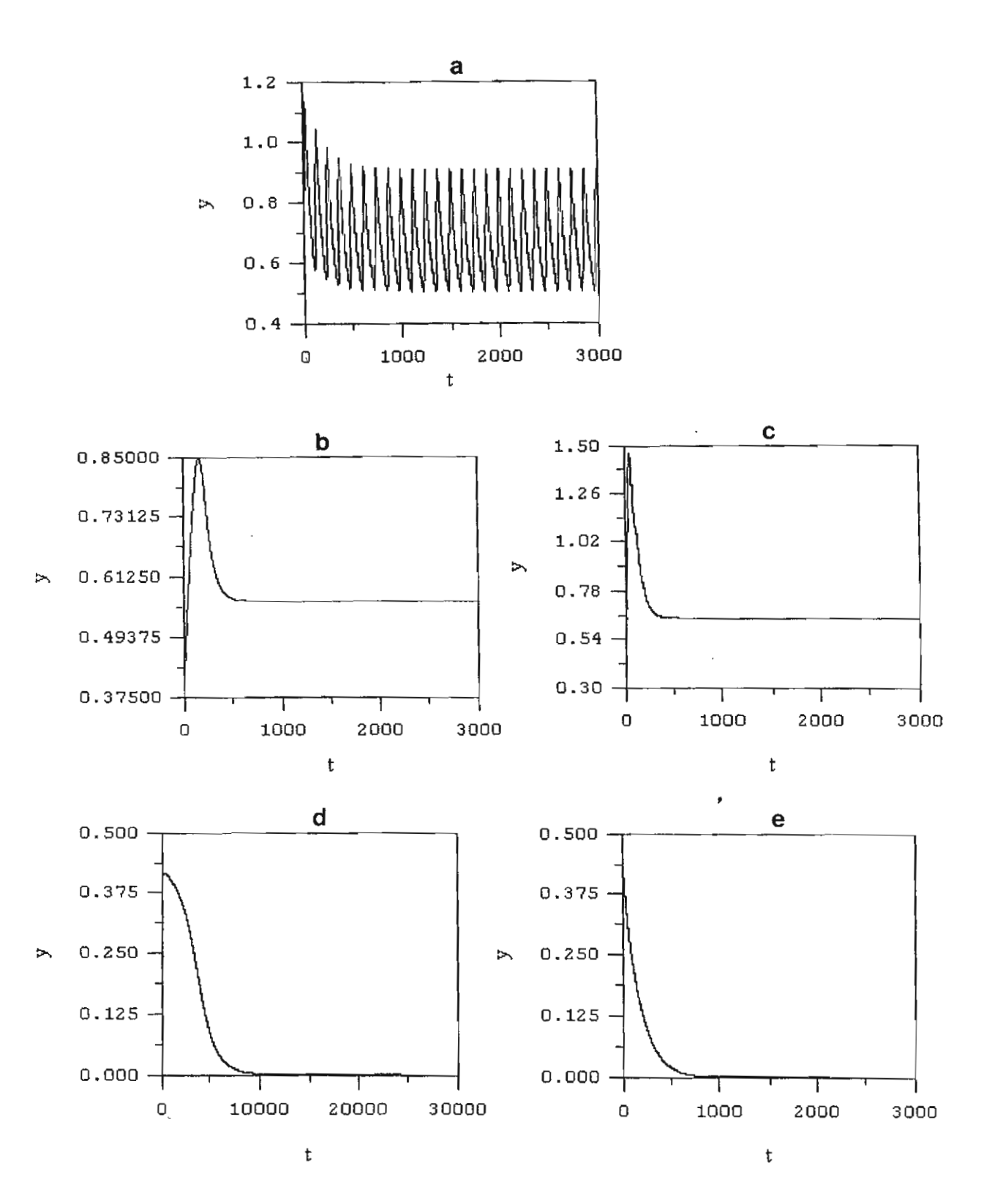


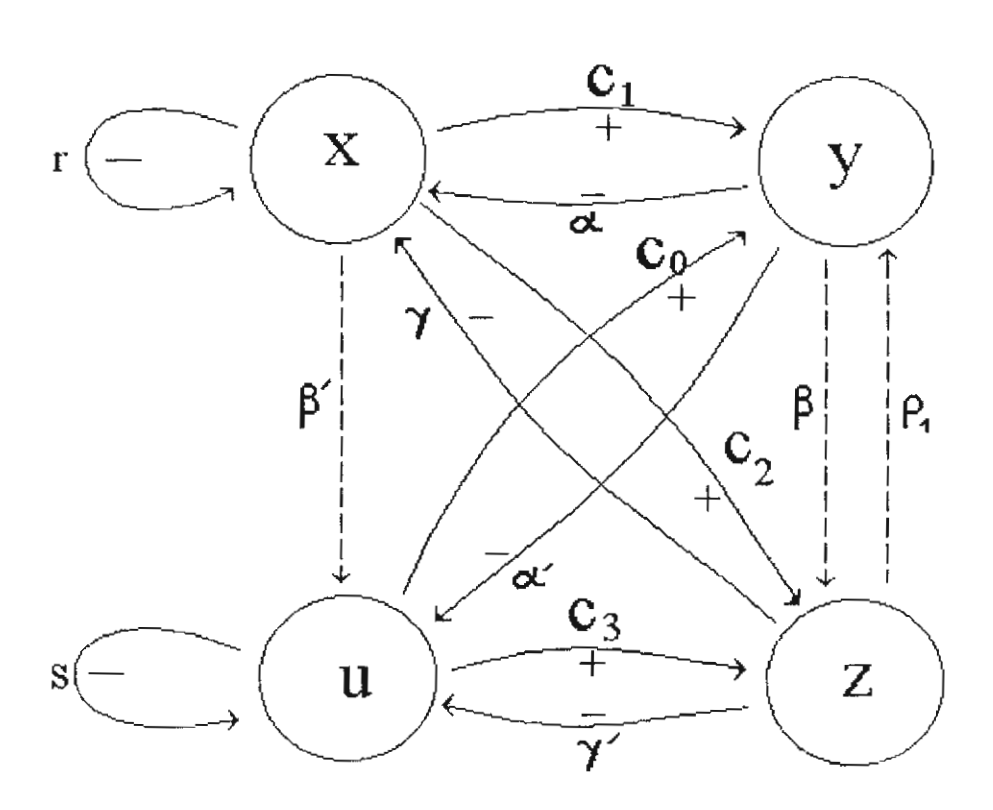


F16.2

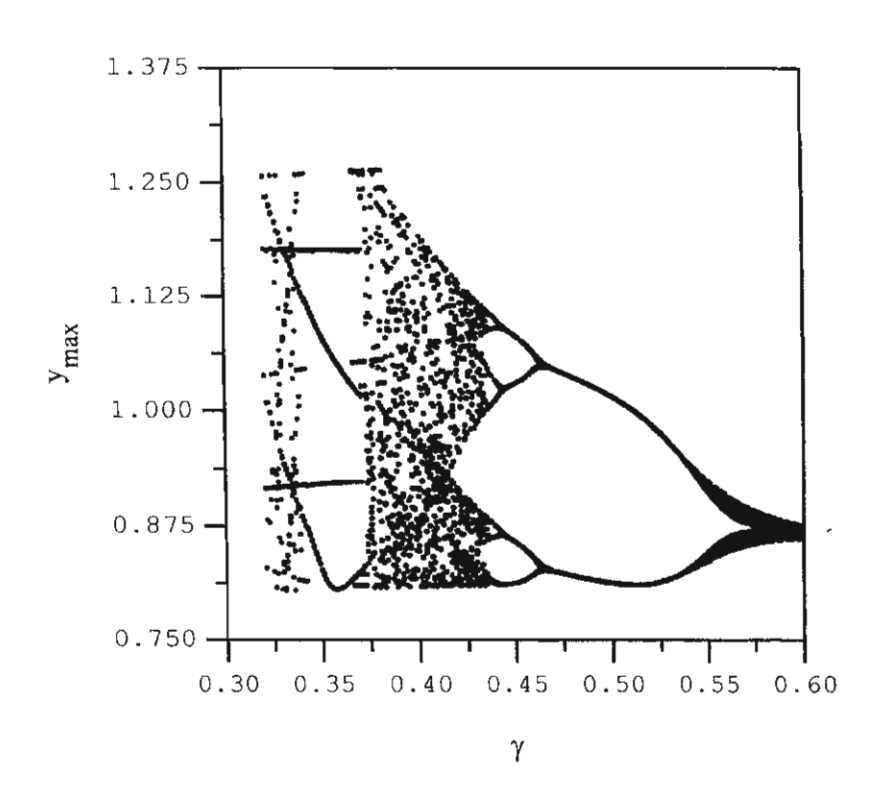




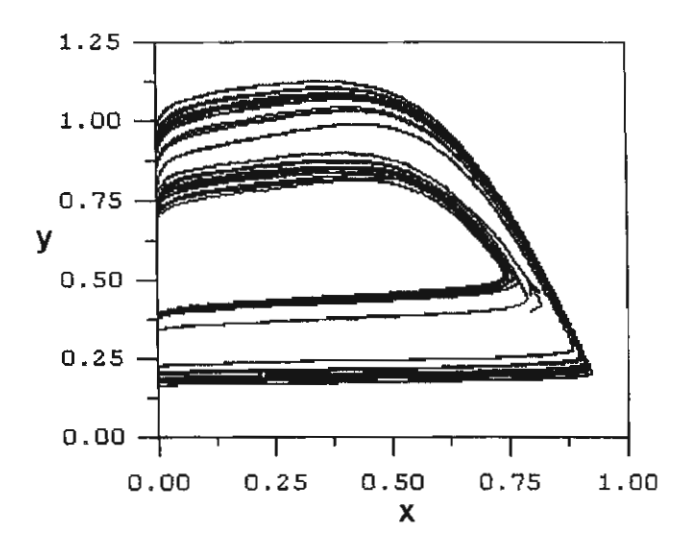


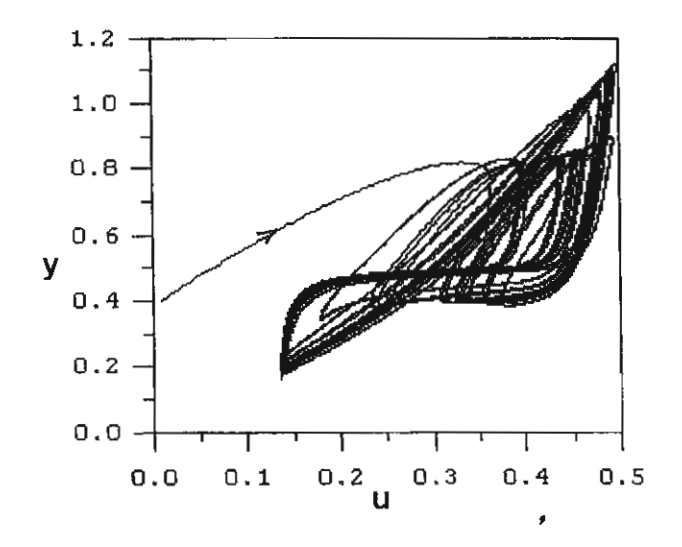


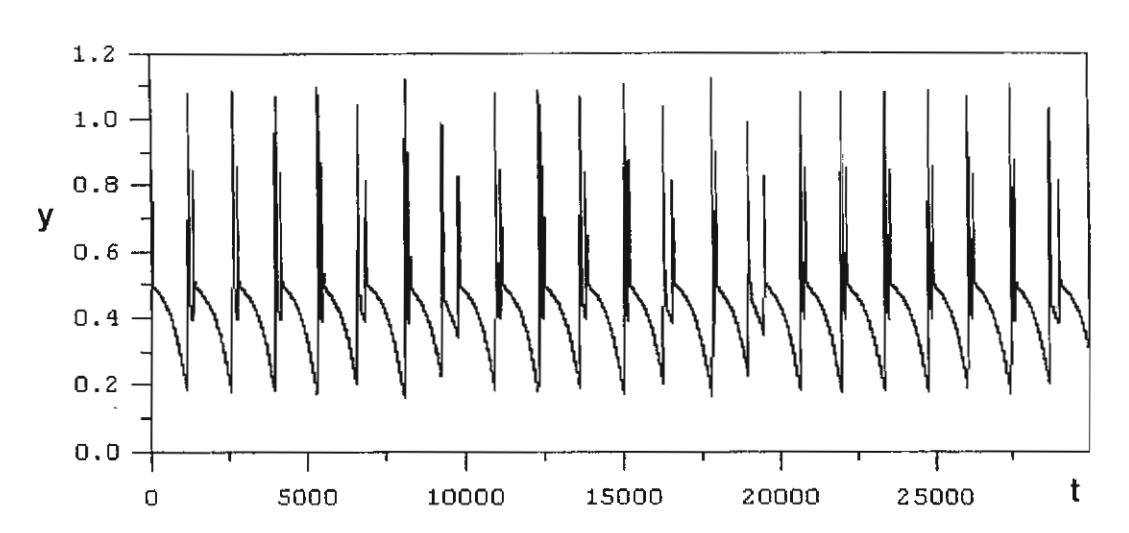
FIEIC



£16.p







F16-7



CHAOS AND CONTROL ACTION IN A KOLMOGOROV TYPE MODEL FOR FOOD WEBS WITH HARVESTING OR REPLENISHMENT

Yongwimon Lenbury*

Adoon Pansuwan

Nardtida Tumrasvin

Department of Mathematics
Faculty of Science, Mahidol University
Rama 6 Rd., Bangkok 10400
THAILAND

Fax: (662) 247-7050

Email: scylb@mahidol.ac.th

^{*} to whom all correspondences should be addressed.

CHAOS AND CONTROL ACTION IN A KOLMOGOROV TYPE MODEL FOR FOOD WEBS WITH HARVESTING OR REPLENISHMENT

Abstract

In this paper, we apply the feedback decoupling technique to a Kolmogorov type model for three species food webs with harvesting or replenishment. A feedback control law is derived to decouple the effect of the predators from the prey dynamics. It is found that the necessary and sufficient conditions for the existence of the decoupling control law rely on the persistence of the prey population and the fact that the specific growth rate of prey depends explicitly on the superpredator population density at any moment in time. It is shown that, without any control action of regulated replenishment or harvesting, irregular or chaotic behavior is possible in such a process for certain ranges of the system parameters. This is illustrated by the construction of a bifurcation diagram for a model of a three-species food web with response functions of the Holling type. To make the system output or variables less sensitive to irregular disturbances, the feedback control technique is applied which produces the desirable effect of stabilizing the system.

1. Introduction

It is possible to classify ecological models as either strategic or tactical, as identified by Holling (1966). The tactical models are relatively more complex. They usually rely on a great amount of supporting data, and are used for making specific predictions. Strategic models, on the other hand, can provide broader insights into possible behaviors of the system based on simple assumptions (McLean and Kirkwood, 1990),

such as the model considered by Hadeler and Freedman (1989) for predator-prey populations with parasitic infection, or the model of continuous bioreactor analyzed by Lenbury and Orankitjaroen (1995).

As Mosetti (1992) has observed, the control of ecological systems for management purposes is a difficult task due to the amount of supporting data needed as well as the conficting management goals. In this respect, a simple reduced strategic model which requires fewer data for calibration can be quite a useful tool when used as a building block for the study of real problems in order to give a decision-maker some preliminary results.

The Kolmogorov model of population growth is, mathematically, probably the most general model of the types considered to date. It incorporates the principle that the growth rate of species is proportional to the number of interacting species present. The classical ecological models of interacting populations typically have focussed on two species. The first Kolmogorov model, developed in 1936, was expanded on by serveral researchers, including May (1972) and Albrecht *et al.* (1974). Such models have been applied to plant and animal dynamics both in aquatic and terrestrial environments (Hastings and Powell, 1991). However, mathematical developments reveal that community models involving only two species as the building blocks may miss quite a great deal of important ecological behavior. In fact, it is now recognized that in community studies the essence of the behavior of a complex system may only be understood when attempts are made to incorporate the interactions among a larger number of species.

Researchers of the last decade or so have turned their attention to the theoretical study of food webs as the "building blocks" of ecological communities and have been faced with the problem of how to couple the large number of interacting species. Behavior of the entire community is then assumed to arise from the coupling of strongly interacting pairs. The approach is attractive by its virtue of being tractable to theoretical analysis (Hastings and Powell, 1991). Yet, many researchers have demonstrated that very complex dynamics can arise in model systems with three species (Gilpin, 1979; Rai and Sreenivasan, 1993). For example, an investigation by Hastings and Powell (1991) showed

that a continuous time model of a food chain incorporating nonlinear functional (and numerical) responses can exhibit chaotic dynamics in long-term behavior when reasonable parametric values are chosen. The key feature observed in chaotic dynamics is the sensitive dependence on initial conditions.

In this paper, we first study the possibility of making the ecosystem output or variables less sensitive to irregular disturbances by applying the feedback control technique in order to stabilize the system. A feedback control law is derived to decouple the effect of the predators from the prey dynamics in a three-species food web of Kolmogorov type. It is found that the necessary and sufficient conditions for the existence of the decoupling control law rely on the persistence of the prey population and the fact that the specific growth rate of prey depends explicitly on the superpredator population density at any moment in time.

We demonstrate by the construction of a bifurcation diagram for a model with response functions of the Holling type that, without any control action, chaotic behavior may result through period doubling bifurcations. Once, the feedback decoupling control action is in place, the system can be stabilized and in this context we obtain a process which is more easily controllable.

2. The Kolmogorov Type Model and the Static Decoupling Problem

We consider a general Kolmogorov type model of n-species food webs, which may be written as follow

$$\dot{X}_i = X_i F_i + U_i$$
 , $i = 1, 2, ..., n$ (1)

where X_i is the *i-th* species population density, U_i is the input/removal (replenishment/harvesting) rate of the *i-th* species, and

$$F_i = F_i(X_1, X_2, ..., X_n)$$
, $i = 1, 2, ..., n$

Such a system (1) can be used to model population dynamics of plant or animal interactions in an aquatic or terrestorial environment such as in the work of Lenbury and Siengsanan (1993), where an activated sludge process was analyzed using a 3-species Kolmogorov type model. Also, in the study by Lenbury and Likasiri (1994) the dynamic behavior of a model for a food web was investigated through the application of the singular purterbation technique.

To formulate the static feedback decoupling problem, we let

$$X = (X_1 \ X_2 \ \dots \ X_n)^t$$

$$F = (F_1 \ F_2 \ \dots \ F_n)$$

$$U = (U_1 \ U_2 \ ... \ U_{n-1})^t$$

and

$$G(X) = \begin{pmatrix} 1 & 0 & 0 & \cdots & 0 \\ 0 & 1 & 0 & \cdots & 0 \\ \cdot & \cdot & \cdot & \cdots & \cdot \\ \cdot & \cdot & \cdot & \cdots & 0 \\ 0 & 0 & 0 & \cdots & 1 \\ 0 & 0 & 0 & \cdots & 0 \end{pmatrix}$$

an $(n-1) \times n$ matrix. Then, the system of equations (1) with $u_n = 0$ can be rewritten as

$$\dot{X}_i = X_i F_i + [GU]_i$$
, $i = 1, 2, ..., n$ (2)

The output of equation (2) is then assumed to be

$$Y = (X_n \ X_2 \ \dots \ X_{n-1})^t \equiv H(X)$$
 (3)

The static feedback decoupling problem, as stated in the work by Mosetti (1992) and explained in greater detail by Isidori (1985), can be defined as follows. "Given equations (2) and (3), we need to find a feedback law $\alpha(X)$ and a state-dependent change of coordinates $\beta(X)$ in the input space \Re^n such that the closed-loop system formed by the combination of (2) and (3) with the control law

$$U = \alpha(X) + \beta(X)V$$

has the *i-th* output dependent only on the *i-th* component of the new input V".

In order to accomplish this, we introduce the following notation. Letting

$$\nabla^* = \left(X_1 \frac{\partial}{\partial X_1} \quad X_2 \frac{\partial}{\partial X_2} \quad \cdots \quad X_n \frac{\partial}{\partial X_n} \right)^t$$

then the operator ∇_F is defined as

$$\nabla_E H_i = F \nabla^* H_i$$

We then understand that

$$\nabla_{E}^{k}H_{i} = \nabla_{F}(\nabla_{E}^{k-1}H_{i})$$

while $\nabla_E^0 H_t = H_t$.

Further, the characteristic number ρ_i associated with the output Y_i can be defined as the largest integer such that for all $k < \rho_i$

$$grad(\nabla_F^k H_i)G_j = 0$$
 , $j = 1, 2, ..., n-1$

where G_j is the *j-th* column of the matrix G.

Accordingly, the decoupling matrix A(X) associated with equations (2) and (3) is the $n \times n$ matrix

$$A(X) = (a_{ij})$$

where

$$a_{ij} = grad(\nabla_F^{\rho_i} H_i)G_i$$

The static state-feedback decoupling theory (Mosetti, 1992) then states that

$$\alpha(X) = -A^{-1}(X)J$$

and

$$\beta(X) = A^{-1}(X)$$

where

$$J = (\nabla_F^{\rho_1+1} H_1, \nabla_F^{\rho_2+1} H_2, ..., \nabla_F^{\rho_n+1} H_n)^t$$

provided that the decoupling matrix A(X) is nonsingular.

3. Application to Three Species Food Webs

3.1 THE CONTROL LAW

We now derive the control law for the Kolmogorov type model for a three species food web which can be written as

$$\dot{x} = x f(x, y, z) + u_1 \tag{4}$$

$$\dot{y} = y g(x, y, z) + u_2 \tag{5}$$

$$\dot{z} = z \ h(x, y, z) \tag{6}$$

where z is the prey population density, y and x are the predator and superpredator, respectively, while u_1 and u_2 are the corresponding input rates. Then,

$$X = \begin{pmatrix} x & y & z \end{pmatrix}^t$$

$$F = (f \quad g \quad h)$$

$$U = \begin{pmatrix} u_1 & u_2 \end{pmatrix}^t$$

$$G(X) = \begin{pmatrix} 1 & 0 \\ 0 & 1 \\ 0 & 0 \end{pmatrix}$$

and the output is

$$Y = H(X) = \begin{pmatrix} z & y \end{pmatrix}^t \tag{7}$$

The main result of the static state-feedback decoupling theory can be stated as follows.

Theorem A necessary and sufficient condition for the existence of (α, β) which solves the decoupling problem for equations (4)-(6) is that the prey population persists and the specific growth rate of prey h depends explicitly on the superpredator population density. If this is the case, then a possible decoupling control is given by:

$$\alpha(X) = \left(-xf - \frac{h}{h_x}(zh_z + h) - yg\right)^t$$

$$\beta(X) = \begin{pmatrix} \frac{1}{zh_x} & -\frac{h_y}{h_x} \\ 0 & 1 \end{pmatrix}$$

and

$$u_1 = -xf - \frac{h}{h_x}(zh_z + h) + \frac{1}{zh_x}v_1 - \frac{h_y}{h_x}v_2$$
 (8)

$$u_2 = -yg + v_2 \tag{9}$$

Proof From its definition, we can show that $\rho_1 = 1$ and $\rho_2 = 0$. We then find that

$$\nabla^* H_1 = \begin{pmatrix} 0 & 0 & z \end{pmatrix}^t$$

so that $\nabla_F^1 H_1 = zh$, and $\nabla_F^0 H_2 = y$. Therefore, we obtain

$$A(X) = \begin{pmatrix} zh_x & zh_y \\ 0 & 1 \end{pmatrix} \tag{10}$$

Thus, A(X) is nonsingular if and only if $\det A \neq 0$, namely

$$zh_{x} \neq 0 \tag{11}$$

This leads to the requirement that prey persists, in which case z > 0, and that $h_x \neq 0$ or, equivalently, h depends explicitly on x.

If we now let

$$\xi = \frac{dz}{dt} \tag{12}$$

then, since $\dot{z} = zh$, we have

$$\frac{d\xi}{dt} = \frac{\partial(zh)}{\partial x}\dot{x} + \frac{\partial(zh)}{\partial y}\dot{y} + \frac{\partial(zh)}{\partial z}\dot{z}$$

$$= zh_x(xf + u_1) + zh_y(yg + u_2) + (zh_z + h) = v_1$$

by applying the law in equations (8) and (9). Also, using (9), we find

$$\frac{dy}{dt} = yg + u_2 = v_2$$

Therefore, in the new coordinate system (ξ, y, z) we have

$$\frac{d\xi}{dt} = v_1 \tag{13}$$

$$\frac{dy}{dt} = v_2 \tag{14}$$

$$\frac{dz}{dt} = \xi \tag{15}$$

which clearly shows the decoupled structure, namely, each of the control variables acts only on one state variable. In fact, to keep the system decoupled, one approach is to set $v_1 = 0$. Then, ξ now remains constant, say at $\xi(t_0)$.

Integrating (15), we obtain

$$z(t) = \xi(t_0)t + z(t_0)$$

Thus, if $\xi(t_0) = 0$ at a given initial time $t = t_0$ when the control is activated, then

$$z(t) = z(t_0)$$

for all subsequent time t, whatever the fluctuation of v_2 . This means that the prey population will not depend upon variations in the predator or superpredator. This is the essential feature of this technique, whereby the variations in the predator and superpredators are decoupled from the prey dynamics.

3.2 PERSISTENCE CONDITIONS

The question of persistence has been dealt with in various literature in all its versions: weak persistence; strong persistence; and uniform persistence (Huaping and Zhien, 1991). We shall give, in the following Lemma, the persistence conditions for the standard food web consisting of equations (4)-(6) with

$$f(x,y,z) = \left(\frac{c_2 y}{b_2 + y} + \frac{c_3 z}{b_3 + z} - d\right)$$
 (16)

$$g(x, y, z) = \left(\frac{c_1 z}{b_1 + z} - \frac{a_2 x}{b_2 + y} - d\right)$$
 (17)

$$h(x, y, z) = r(1 - \frac{z}{k}) - \frac{a_1 y}{b_1 + z} - \frac{a_3 x}{b_3 + z}$$
(18)

where d is the specific removal rate, and the terms

$$\frac{a_i z}{b_i + z} \quad , \qquad i = 1, 3$$

and

$$\frac{a_2y}{b_2+y}$$

are the population response functions of the Holling type in which a_i is the maximum predation rate and b_i is the so-called half-saturation constant. The construction and analysis of the model in the cae that $u_1 = u_2 = 0$ may be found in the work of Lenbury and Likasiri (1994).

A standard food web given by equations (4)-(6) with (16)-(18) generally posesses only one positive equilibrium $\hat{E} = (0, \hat{y}, \hat{z})$ and possibly only one positive limit cycle $\hat{\Gamma} = (0, \hat{y}(t), \hat{z}(t))$ for its subsystem (5)-(6) with x set equal to zero. Under this assumption, we are led to the following Lemma.

Lemma The food web given by equations (4)-(6) with (16)-(18) is persistent if \dot{x} is positive for small x in the vicinity of \hat{E} and $\hat{\Gamma}$, that is if

$$\frac{c_2\hat{y}}{b_2+\hat{y}} + \frac{c_3\hat{z}}{b_3+\hat{z}} > d \tag{19}$$

and (in the case that $\hat{\Gamma}$ exists)

$$\frac{1}{T} \int_0^T \left(\frac{c_2 \hat{y}(t)}{b_2 + \hat{y}(t)} + \frac{c_3 \hat{z}(t)}{b_3 + \hat{z}(t)} \right) dt > d$$
 (20)

where T is the period of the limit cycle $\hat{\Gamma}$, provided that u_1 and u_2 are identically zero. Otherwise, the population persists if

$$u_1(0, \hat{y}, \hat{z}) > 0$$
 (21)

and (in the case that $\hat{\Gamma}$ exists)

$$\frac{1}{T} \int_{0}^{T} u_{1}(0, \hat{y}(t), \hat{z}(t)) dt > 0$$
 (22)

Proof Since the superpredator x of a food web goes extinct if one of the other populations does so, persistence depends on the bahavior of (4)-(6) in the vicinity of the nonwashout equilibria (z>0) and limit cycles of the prey-predator subsystem (5)-(6) with x=0. Therefore, the population persists if the injection of a small number of superpredator gives rise to an invasion of the positive actant $(\dot{x}>0)$ from such equilibria or limit cycles lying on the (y,z) face.

To be precise, using equation (4) with $u_1 = u_2 = 0$, \dot{x} will be positive for small x in the vicinity of \hat{E} and $\hat{\Gamma}$ if

$$f\Big|_{\hat{E}} > 0 \tag{23}$$

and (in the case that $\hat{\Gamma}$ exists)

$$\frac{1}{T} \int_0^T f(0, \hat{y}(t), \hat{z}(t)) dt > 0$$
 (24)

T being the period of the limit cycle $\hat{\Gamma}$.

On substituting in (23) and (24) for f from equation (16), we arrive at the persistence conditions (19) and (20) in the case that u_1 and u_2 are identically zero. If, on the other hand, u_1 and u_2 are not identically zero, persistence is then assured if conditions (21) and (22) hold, assuming that all functions involved are continuous.

Consequently, on substituting (16)-(18) into (8) and (9), one obtains the following decoupling feedback law.

$$u_{1} = -x \left(\frac{c_{2}y}{b_{2} + y} + \frac{c_{3}z}{b_{3} + z} - d \right)$$

$$+ \frac{z(b_{3} + z)}{a_{3}} \left(r(1 - \frac{z}{k}) - \frac{a_{1}y}{b_{1} + z} - \frac{a_{3}x}{b_{3} + z} \right) \left(r(1 - \frac{2z}{k}) - \frac{a_{1}b_{1}y}{(b_{1} + z)^{2}} - \frac{a_{3}b_{3}x}{(b_{3} + z)^{2}} \right)$$

$$- \frac{b_{3} + z}{a_{3}z} v_{1} - \frac{a_{1}(b_{3} + z)}{a_{2}(b_{1} + z)} v_{2}$$

$$(25)$$

$$u_2 = -y \left(\frac{c_1 z}{b_1 + z} - \frac{a_2 x}{b_2 + y} - d \right) + v_2 \tag{26}$$

Figure 1 shows the time courses of the three state variables and the discharge rates u_1 and u_2 under normal conditions. We then chose to start our control action at the time $t=t_0$ shown in the Figure where $\dot{z}=\xi(t_0)=0$. Thus, the effect of the control action is seen in Figure 2 when the new input v_1 is set equal to zero and v_2 is taken to be of the form

$$v_2 = Ae^{-\gamma t} \sin \omega t$$

which corresponds to a damped sinusoidal input. The prey population density z becomes constant after the time t_0 , while the predator and superpredator vary in a sinusoidal fashion with damping amplitude. As time passes, the new input rate v_2 becomes negligently small and the corresponding population densities of all three species are maintained at constant levels as a result.

4. Control Action on a Chaotic System

In the work by Lenbury and Likasiri (1994), the model of a food web given by equations (4)-(6) with (16)-(18) and $u_1 = u_2 = 0$ have been analyzed using the singular perturbation method. Explicit conditions were derived which separate the various dynamic structures and identify the limit cycles composed of alternately slow and fast transitions. In particular, it was found that the system will have a unique global attractor in the first octant which is a low-frequency limit cycle with a period of high-frequency oscillation if the following conditions hold on the system parameters.

$$\frac{4a_1b_1b_2c_1k}{(b_1+k)^2} < \frac{r(b_3-b_1)[c_1(k-b_1)-d(b_1+k)]}{2b_3+k-b_1}$$
(27)

$$k(c_1 - d) > b_1(c_1 + d)$$
 (28)

$$\frac{b_2(c_1k - b_1d - dk)}{a_2(b_1 + k)} < \frac{b_1b_3(a_1 + r)[c_1(k - b_3) - d(2b_1 + k - b_3)]}{(a_1b_3 - a_3b_1d)(2b_1 + k - b_3) + a_3b_1c_1(k - b_3)}$$
(29)

and
$$\frac{c_i}{d}$$
 $(i = 1, 2, 3)$ are sufficiently high.

We now carry out a numerical investigation to determine the ranges of parametric values where chaotic dynamics were likely. Our choice of parameters was guided by two factors. First, we follow the example of the work by Lenbury and Likasiri (1994) and assume that the ecological system under study may be characterized by highly diversified dynamics. Accordingly, we chose parametric values so that the time response of the system equations (4)-(6) increases from top to bottom. The prey is assumed to have very fast dynamics, while the predator and superpredator have intermediate and slow dynamics, respectively. Phytoplankton - zooplankton - fish is a typical example of an ecosystem where time response increases with the trophic levels. In fact, most food chains observed in nature have time responses increasing along the chain from top to bottom.

Second, as has been noted by many previous workers (Hastings and Powell, 1991; Rai and Sreenivasan, 1993), one may be able to generate chaos in a nonlinear system which already exhibits limit cycle behavior. We therefore chose parametric values to satisfy the conditions (27)-(29) found by Lenbury and Likasiri (1994) to lead to a solution trajectory on a low frequency limit cycle with bursts of high frequency oscillations.

Our investigation involves letting the system run for 100,000 time steps and examing only the last 80,000 time steps to eliminate transient behavior. We use values of b_1 between 4.0 and 4.5, changing b_1 in steps of 0.01. The relative maximum values x_{max} of x, collected during the last 80,000 time steps, are plotted as a function of b_1 as shown in Figure 3.

We discover in this bifurcation diagram the appearance of a period doubling route to chaos, similar to those exhibited by one-dimensional difference equations such as the logistic population model. Apparently, the system of equations (4)-(6) with (16)-(18) exhibits chaotic dynamics for values of b_1 between 4.22 and 4.32. Windows in the bifurcation diagram are observed for b_1 in the range $4.26 < b_1 < 4.32$ and $4.34 < b_1 < 4.40$, for example, where periodicity is re-established.

Figure 4 shows the solution trajectory of the model system (4)-(6) with (16)-(18) using $b_1 = 4.3$ in the chaotic range identified in the bifurcation diagram. The strange attractor is projected onto the (y,z)-plane in Figure 4, and the corresponding chaotic time courses of x, y, and z in uncontrolled conditions are shown in Figure 5 with the discharge rates u_1 and u_2 .

Figure 6 shows the time courses of z starting from two different initial conditions. The difference in the two starting values of z is merely 0.01. We observe that, while the two plots follow nondistinguishable paths during the initial short period, they begin to diverge and follow noticeably different paths eventually. This demonstrates clearly the sensitivity to initial conditions which is the essential characteristic of chaotic behavior.

Figure 7 then shows the effect of the control action on the chaotic system of Figure 4 with v_1 set equal to zero and v_2 chaotic. Here, the control is initiated at the point where $\dot{z}(t_0) = 0$ and $\ddot{z}(t_0) < 0$. Once the control action is in place, prey is maintained at a

constant high level, while the variations in predator, superpredator, and the discharge rates u_1 and u_2 are irregular.

On applying the model to an activated sludge process, the state variables can be nutrient-bacteria-protozoa, for example, and the objective of the control action is perhaps to regulate the inputs in order to obtain satisfactory water quality. In such a case, it is desirable to start the control action when the variable z falls to its first lowest point $(\dot{z}(t_0) = 0)$ and $\ddot{z}(t_0) > 0$. We will then be able to maintain z at a constant low level.

5. Conclusion

It has been demonstrated that while some inherent properties of a nonlinear model permit the emergence of chaotic dynamics, they also allow the existence of a feedback decoupling control mechanism. Since the behavior of the entire community is believed to arise from the coupling of these strongly interacting species, the detection and possibility of control of a chaotic system is of critical importance. If a generalization from a food web model depends cricially upon behavior after a long time, then the role of chaos may be extremely relevant.

On a cautious note, the question of whether or not deterministic chaos actually occurs in a real ecosystem is still open to discussions. As has been observed by Sabin and Summers (1993), "... there is still no generally accepted example of a chaotic ecosystem in nature. Moreover, some traditional ecologists believe that irregular oscillations in natural populations are attributed to random perturbations or noise in the environment rather than being the result of the intrinsic nonlinear dynamics of the system."

Perhaps the first concrete example of occurrence of chaos in nature is due to Sugihara and May (1990) who showed that there underlies a three-dimensional chaotic attractor in the dynamics of marine planktonic diatoms. Despite of the fact that the corresponding time series is very noisy, they have been able to extract the information which allows them to describe some of the dynamics as deterministic chaos.

Such irregular behavior is not desirable when one is interested in managing a system, since chaos allows only short-term predictions. Thus, a feedback control mechanism such as the one we have been discussing provides an attractive and useful tool to regulate the process since it can stabilize the system and make it less sensitive to the exogeneous disturbances or noise input. The present study has potential to be a spring board for a generalization to more complex models in the hope of obtaining a more manageable system.

Acknowledgement

Appreciation is rendered to the Thailand Research Fund and the National Research Council of Thailand for the financial support which has made possible this research project.

References

Albrecht, F., Gatzke, A., Haddad, A. & Wax, N. (1974). The dynamics of two interacting populations. *J. Math. Anal. Appl.* **46**, 658-670.

Gilpin, M. E. (1979). Spiral chaos in a predator-prey model. *American Naturalist*. 107, 306-308.

Hadeler, K. P. & Freedman, H. I. (1989). Predator-prey populations with parasitic infection. *J. Math. Biol.* **28**, 609-631.

Hastings, A. & Powell, T. (1991). Chaos in a three-species food chain. *Ecology*.72(3), 896-903.

Holling, C. S. (1966). In *Systems Analysis in Ecology* (Watt, K. E. F., ed.) p. 195. New York: Academic Press.

Huaping, L. & Zhien, M. (1991). The threshold of survival for system of two species in a polluted environment. *J. Math. Biol.* **30**, 46-61.

Isidori, A. (1985). (1985). *Non-linear Control Systems: An Introduction*. Springer Lecture Notes in Control and Information Sciences. 297 pp. Berlin: Springer-Verlag.

Lenbury, Y. & Orankitjareon, S. (1995). Dynamic behavior of a membrane permeability sensitive model for a continuous bio-reactor exhibiting culture rhythmicity. *J. Sci. Soc. Thailand.* **21**, 97-116.

Lenbury, Y. & Siengsanan, M. (1993). Coexistence of competing microbial species in a chemostat where on population feeds on another. *Acta Biotechnol.* **13**, 1-18.

Lenbury, Y. & Likasiri, C. (1994). Low- and high-frequency oscillations in a food chain where one of the competing species feeds on the other. *Mathl. Comput. Modelling.* **20**(7), 71-89.

May, R. M. (1972). Limit cycles in predator-prey communities. Science. 177, 900-902.

McLean, A. R. & Kirkwood, T. B. L. (1990). A model of human immunodeficiency virus in T helper cell clones. *J. theor. Biol.* **147**, 177-203.

Mosetti, R. (1992). On the control of phytoplankton growth via a decoupling feedback law. *Ecol. Model.* **62**, 71-81.

Muratori, S. & Rinaldi, S. (1992). Low- and high-frequency oscillations in three dimensional food chain systems. *SIAM J. APPL. MATH.* **52**(6), 1688-1706.

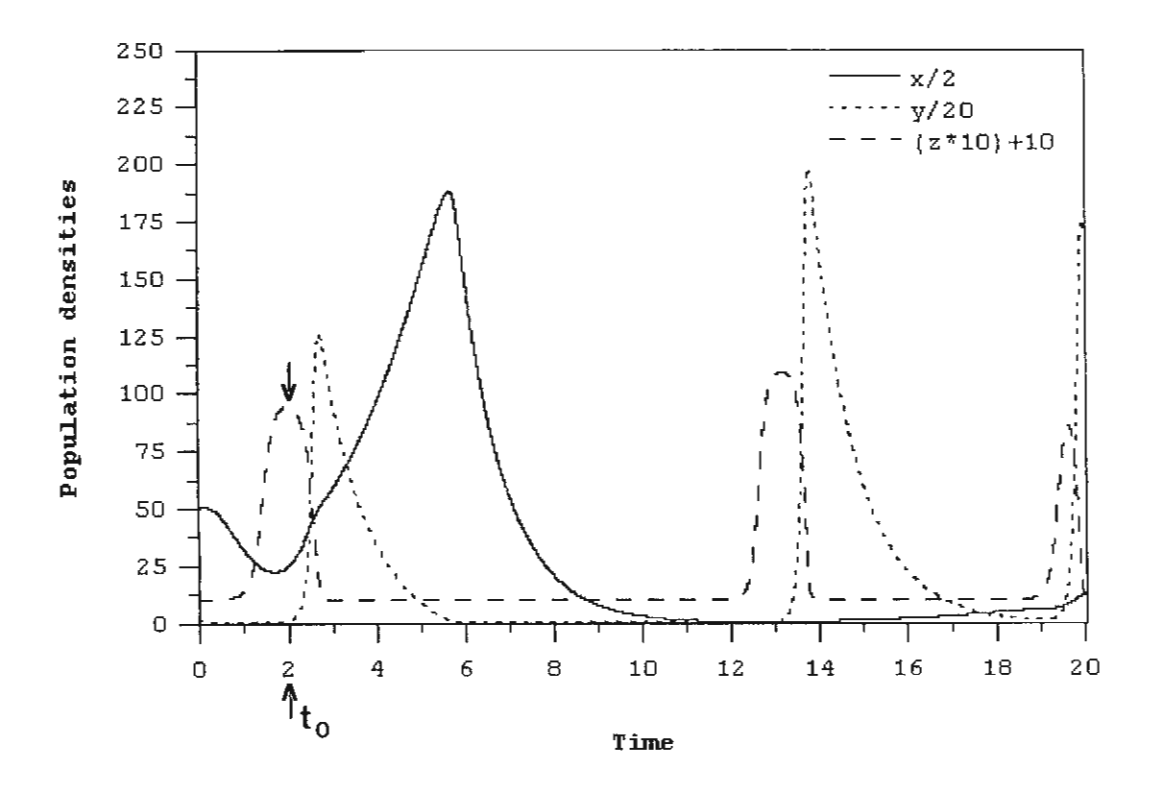
Rai, V. & Sreenivasan, R. (1993). Period-doubling bifurcations leading to chaos in a model food chain. *Ecol. Model.* **69**, 63-77.

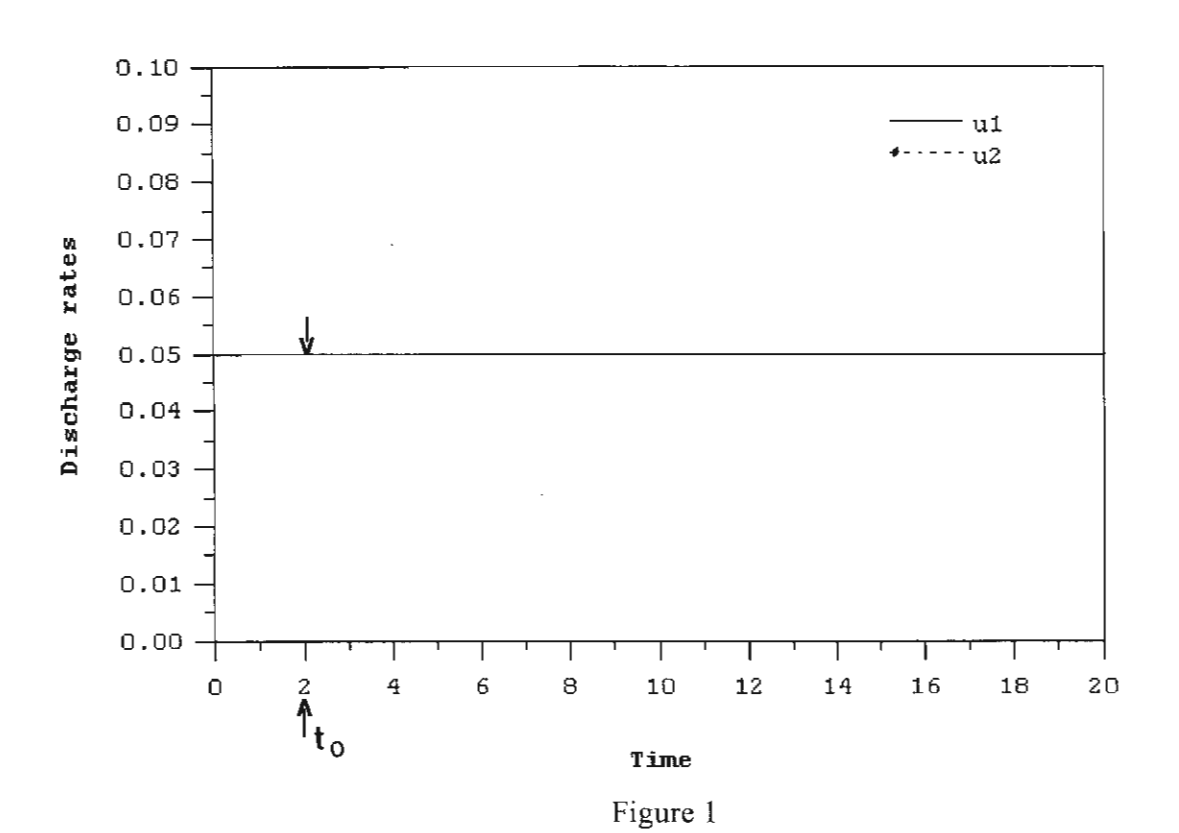
Sabin, G. C. W. & Summers, D. (1993). Chaos in a periodically forced predator-prey ecosystem model. *Math. Biosci.* **113**, 91-113.

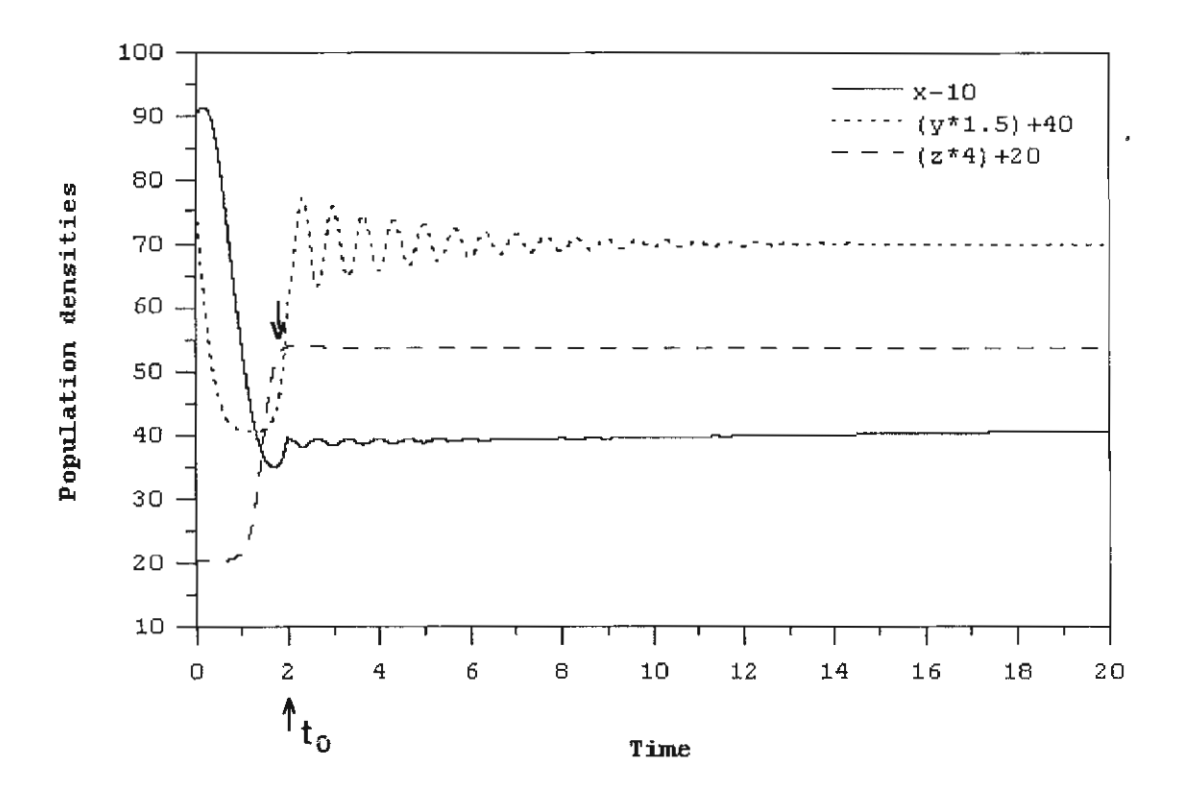
Sugihara, G. & May, R. M. (1990). Nonlinear forcasting as a way of distinquishing chaos from measurment error in time series. *Nature*. **344**, 734-741.

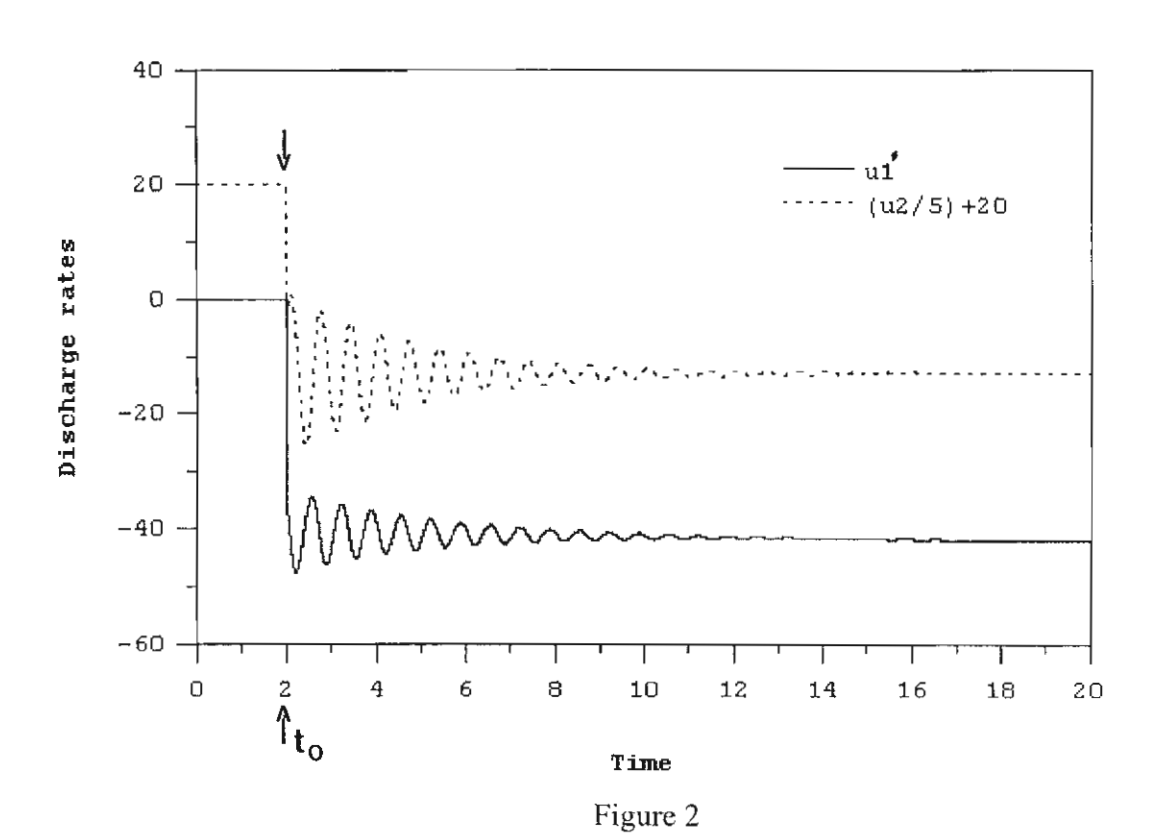
FIGURE CAPTION

- Figure 1 Time evolution of superpredator x (——), predator y (-----), and pery z (----), and constant discharge rates u_1 and u_2 with no control action. Here, $a_1 = 0.05$, $a_2 = 0.5$, $a_3 = 0.5$, $b_1 = 4.0$, $b_2 = 8.0$, $b_3 = 8.0$, $c_1 = 15.0$, $c_2 = 1.5$, $c_3 = 1.5$, d = 1.0, k = 10.0, r = 10.0, $u_1 = 0.005$, and $u_2 = 0.005$.
- Figure 2 Time evolution of superpredator x, predator y, and pery z, and discharge rates u_1 and u_2 under control operations starting at $t = t_0$ with $v_1 = 0$ and $v_2 = 100e^{-t/3} \sin 3\pi t$, and the system parameters as in Figure 1.
- Figure 3 Bifurcation diagram for the model system (4)-(6) with (16)-(18), using the value of b_1 from 4.0 to 4.5, and other parametric values as in Figure 1. Plots are of the relative maximum values of x vs. b_1 .
- Figure 4 Projection onto the (y,z)-plane of the strange attractor obtained on simulating the model system (4)-(6) with (16)-(18) using $b_1 = 4.3$ in the chaotic range identified in the bifurcation diagram, and other parametric values as in Figure 1.
- Figure 5 Time courses of the three state variables exhibiting chaotic behavior when there is no control action, and parametric values are as in Figure 4.
- Figure 6 Divergence of trajectories when the system exhibits chaotic dynamics. Prey trajectories are plotted for two different initial conditions (—— and -----), differing only by 0.01 in z.
- Figure 7 Time evolution of the three state variables, using parametric values of Figure 5. The chaotic system becomes stabilized when the control action is initiated at $t = t_0$ with $v_1 = 0$ and v_2 irregular.









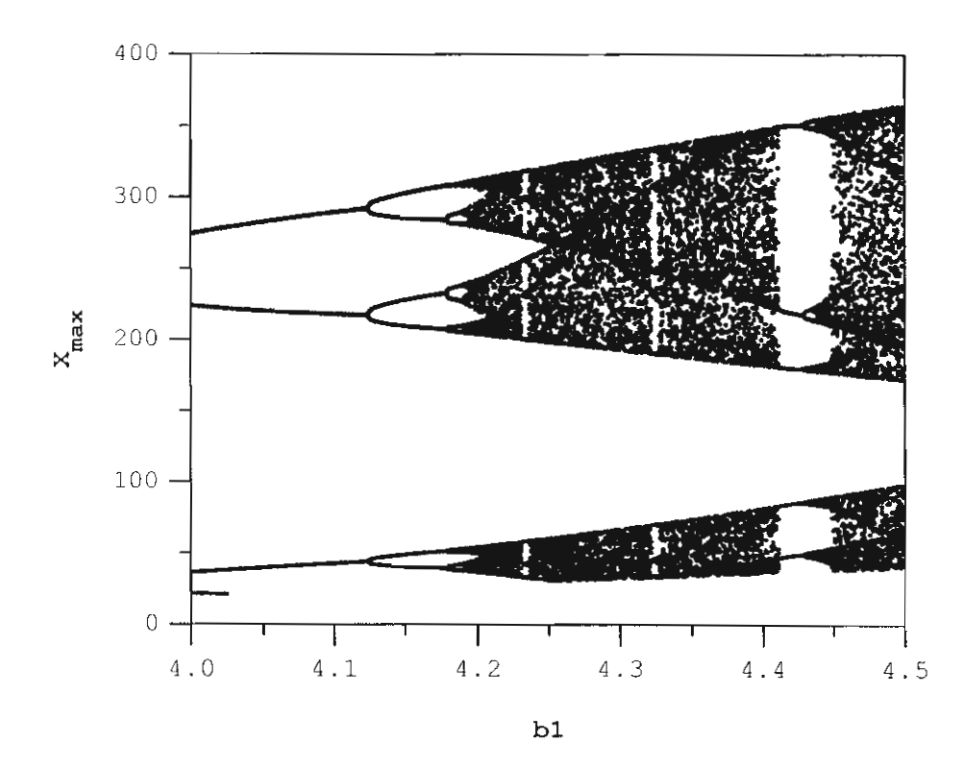


Figure 3

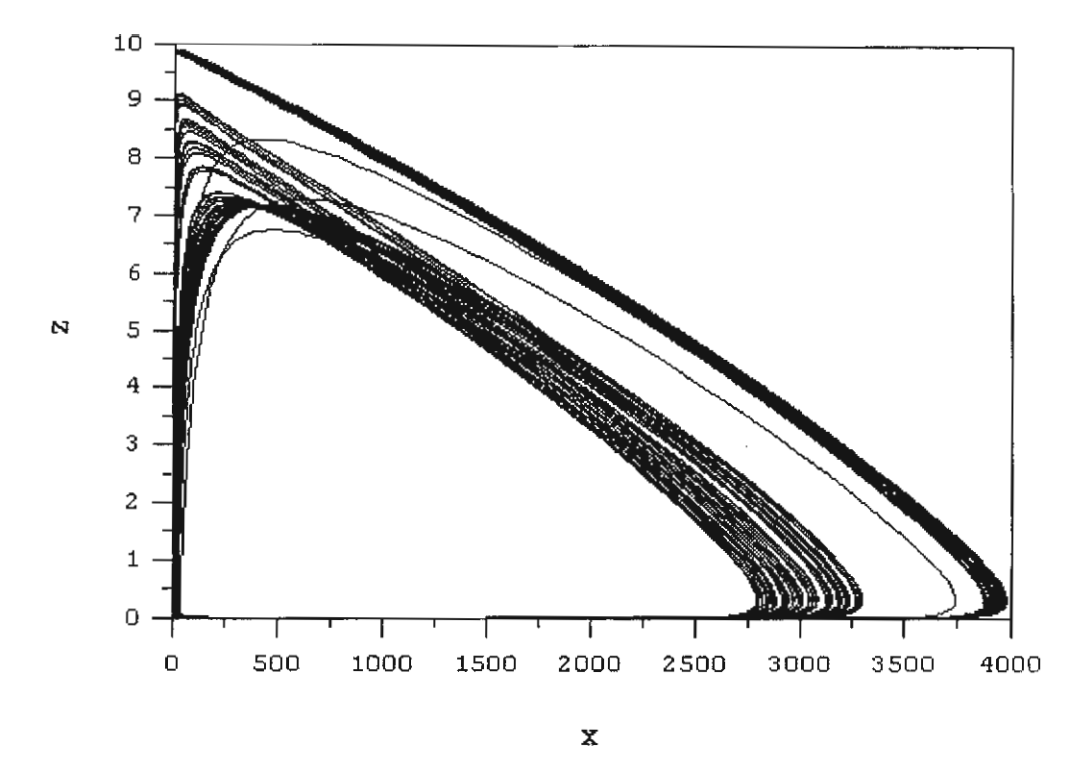
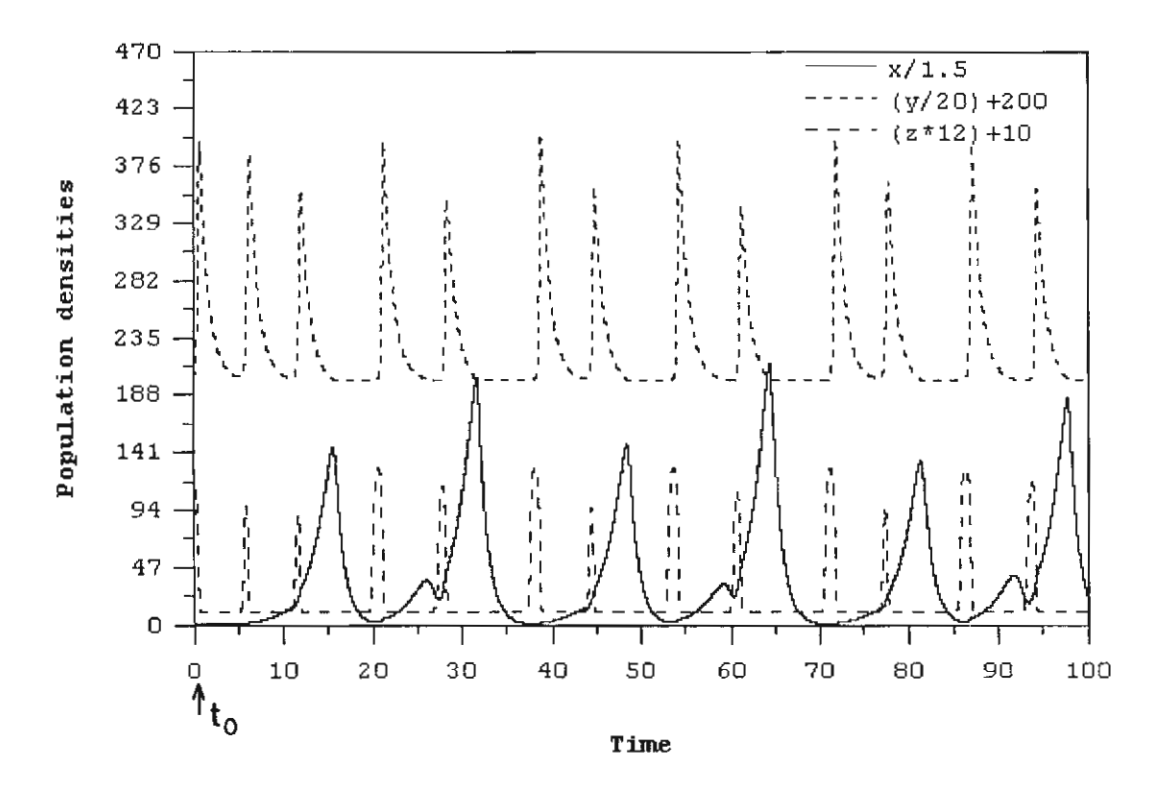
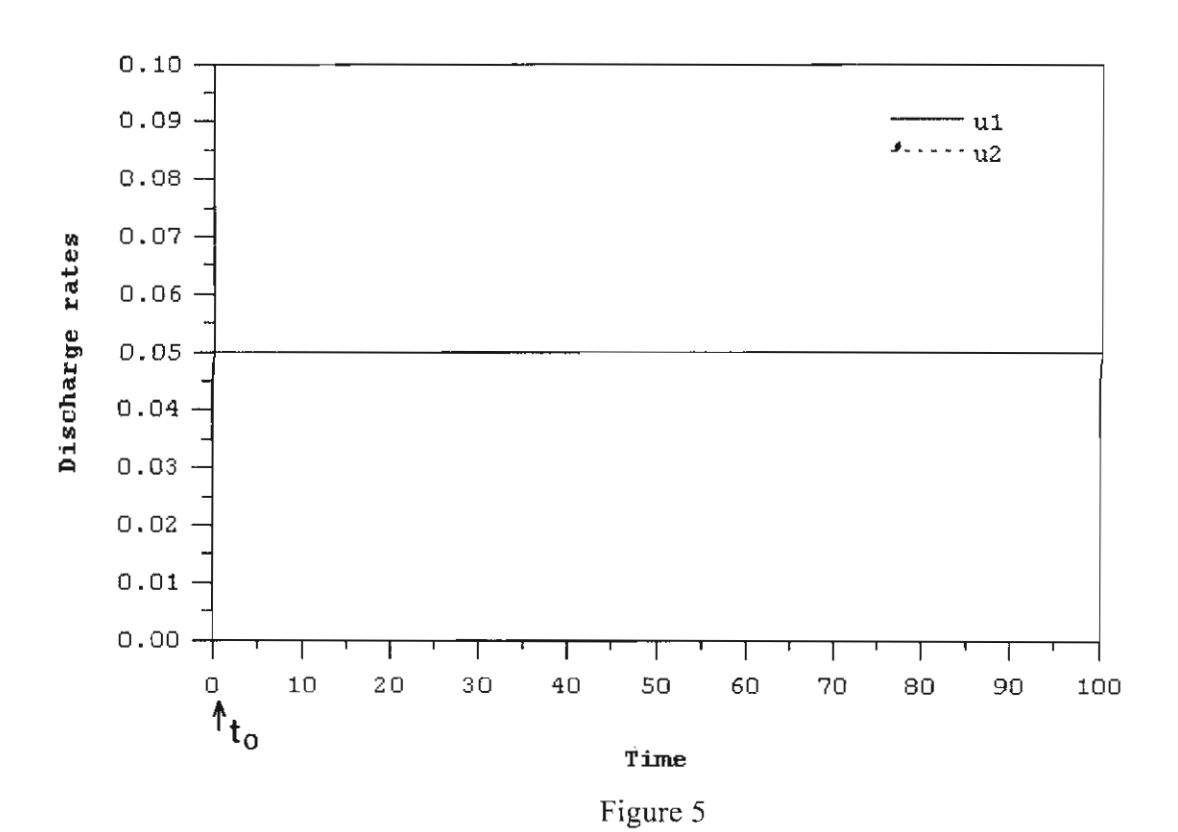


Figure 4





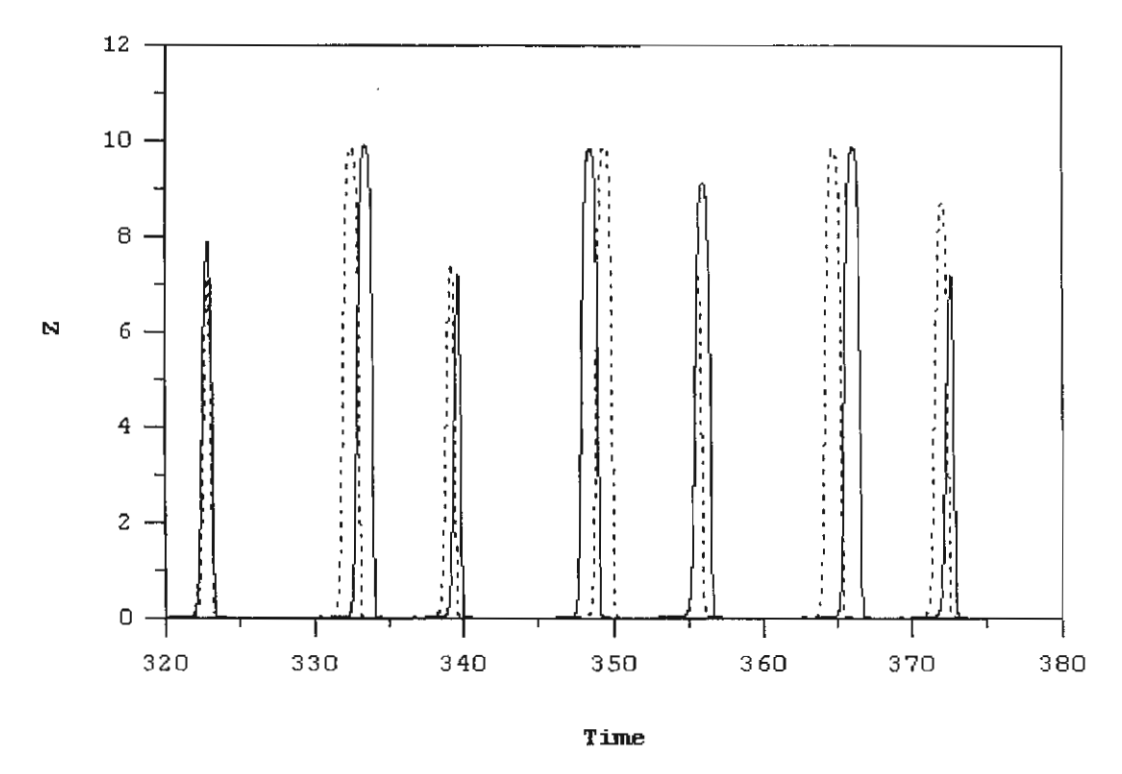


Figure 6

